Group 13 and Lanthanide Complexes Supported by Tridentate Tripodal Triamine Ligands: Structural Diversity and Polymerization Catalysis

Hongping Zhu and Eugene Y.-X. Chen*

Department of Chemistry, Colorado State University, Fort Collins, Colorado 80523-1872

Received June 14, 2007

Several different synthetic approaches to a total of 13 novel B, Al, and Sm complexes derived from the tridentate tripodal triamine ligand $[N_3]H_3$ with a neopentane, trisilylmethane, or trisilylsilane backbone and different *N*-substituents, as well as applications of the selected complexes to polymerization catalysis, are reported. Salt metathesis between $HC[SiMe_2N(CH_2Ph)]_3Li_3(THF)_2$ (THF = tetrahydrofuran) and $AlCl_3$ in Et_2O/hexanes leads to complete elimination of LiCl and formation of the corresponding tripodal triamido alane $HC[SiMe_2N(CH_2Ph)]_3Al\cdot(THF)$ (**1**). On the other hand, the reaction of $\{MeC[CHN(SiMe_3)]_3Li_3\}_2$ and $AlCl_3$ in Et_2O/hexanes yields a LiCl-containing compound $MeC[CH_2N(SiMe_3)]_3AlCl[Li(Et_2O)]$ (**2**). Alkane elimination involving $[N_3]H_3$ and 1 $AlMe_3$ produces diamido−amino aluminum methyl $HC[SiMe_2NHAr][SiMe_2NAr]_2AlMe$ [Ar = 4-MeC_6H_4 (**3**), CH_2Ph (**4**)], while the reaction using ≥2 $AlMe_3$ gives amido−amino aluminum dimethyl $[ArHNMe_2Si](H)C[SiMe_2NAr]_2(AlMe_2)_2$ (Ar = 4-MeC_6H_4, **5**) and $[(Me_3Si)HNCH_2](Me)C[CH_2N(SiMe_3)]_2(AlMe_2)_2$ (**6**). The H_2-elimination route involves treatment of $[N_3]H_3$ with $LiAlH_4$ and AlH_3, affording $[\{HC[SiMe_2N(4\text{-}MeC_6H_4)]_3AlH\}Li]_2$ (**7**) and $MeSi[SiMe_2N(4\text{-}MeC_6H_4)]_3AlH(AlH_2)$ (**8**), respectively. There is no reaction between $[N_3]H_3$ and $Al[N(SiMe_3)_2]_3$; however, the amine-elimination reaction using $Sm[N(SiMe_3)_2]_3$ produces tripodal triamido Sm complex $\{MeSi[SiMe_2N(4\text{-}MeC_6H_4)]_3Sm\}_2$ (**9**). Ligand exchange between tripodal borane $HC[SiMe_2N(4\text{-}MeC_6H_4)]_3B$ and AlR_3 (R = Me, H) offers the first-step ligand exchange product $HC[SiMe_2N(4\text{-}MeC_6H_4)]_3BMe(AlMe_2)$ (**10**) or the second-step ligand exchange product $HC[SiMe_2N(4\text{-}MeC_6H_4)]_3AlH(BH_2)$ (**11**). Activation of dimethyl metallocenes $LZrMe_2$ by $HC[SiMe_2N(4\text{-}MeC_6H_4)]_3B$ produces ligand redistribution products $LZrMe[N(4\text{-}MeC_6H_4)SiMe_2](H)C[SiMe_2N(4\text{-}MeC_6H_4)]_2BMe$ [L = Cp_2 (**12**), *rac*-$Et(Ind)_2$ (**13**)]. Besides characterizations by NMR and elemental analysis of the above new complexes, six of them (**2**, **4**, **5**, **8**, **9**, and **13**) have also been structurally characterized by X-ray single-crystal diffraction studies. "Activated" metallocene complexes **12** and **13** are inactive for ethylene or propylene polymerization. Complex **1** exhibits low activity for ring-opening polymerization (ROP) of propylene oxide, but high activity for ROP of ϵ-caprolactone (CL). Significantly, tripodal aluminum hydride **8** effects catalytic ROP of CL upon addition of benzyl alcohol as a chain-transfer reagent.

Introduction

There has been broad interest in organoboron and aluminum Lewis acids (LAs) since they are essential as reagents, catalysts, cocatalysts, initiators, and scavengers or stabilizers in organic synthesis,[1] olefin polymerization catalysis,[2] and polymerization of polar monomers.[3] A three-coordinate, σ-bound boron or aluminum center, in general, exhibits strong Lewis acidity due to its electron deficiency; however, the formation of partial double bonds between this center and its neighboring atoms can significantly reduce or quench its Lewis acidity. On the one hand, the incorporation of three strongly electron-withdrawing perfluoroaryl ligands, e.g., $E(C_6F_5)_3$ (E = B, Al), further enhances its Lewis acidity as well as the chemical robustness of the resulting anion from the abstractive reaction between such a LA and a transition-metal substrate carrying a basic or nucleophilic ligand.[2] A caveat for the activation process of generating catalytically active ion pairs is the energy penalty paid for the geometry reorganization—from planar triangle to monotrigonal pyramid at the LA center, excluding the abstracted ligand. We viewed this situation as an opportunity for the design of three-coordinate B and Al complexes adopting a *preorganized pyramidal geometry* for enhanced Lewis acidity,[4] based on the reasoning that such a geometry not only provides a vacant sp^3 orbital disposed ideally to accept a fourth donor ligand, but also significantly suppresses the energy penalty for the geometry reorganization during the LA-mediated chemical processes.

On the basis of the above working hypothesis, we[4a] recently reported the synthesis and structure of such pyramidal B and

* To whom correspondence should be addressed. E-mail: eychen@lamar.colostate.edu.

(1) For reviews, see: (a) Ishihara, K. In *Lewis Acids in Organic Synthesis*, Vol. 1; Yamamoto, H., Ed.; Wiley-VCH: Weinheim, Germany, 2000; pp 89−190. (b) Ooi, T.; Maruoka, K. In *Lewis Acids in Organic Synthesis*, Vol. 1; Yamamoto, H., Ed.; Wiley-VCH: Weinheim, Germany, 2000; pp 191−282. (c) Wulff, W. D. In *Lewis Acids in Organic Synthesis*, Vol. 1; Yamamoto, H., Ed.; Wiley-VCH: Weinheim, Germany, 2000; pp 283−354.

(2) For reviews, see: (a) Piers, W. E. *Adv. Organomet. Chem.* **2005**, *52*, 1−76. (b) Erker, G. *Dalton Trans.* **2005**, 1883−1890. (c) Pedeutour, J.-N.; Radhakrishnan, K.; Cramail, H.; Deffieux, A. *Macromol. Rapid Commun.* **2001**, *22*, 1095−1123. (d) Chen, E. Y.-X.; Marks, T. J. *Chem. Rev.* **2000**, *100*, 1391−1434.

(3) For reviews, see: (a) Mecerreyes, D.; Jerome, R.; Dubois, P. *Adv. Polym. Sci.* **1999**, *147*, 1−59. (b) Sugimoto, H.; Inoue, S. *Adv. Polym. Sci.* **1999**, *146*, 39−119. (c) Kuran, W. *Prog. Polym. Sci.* **1998**, *23*, 919−992.

(4) (a) Zhu, H.; Chen, E. Y.-X. *Inorg. Chem.* **2007**, *46*, 1481−1487. (b) Jansen, G.; Schubart, M.; Findeis, B.; Gade, L. H.; Scowen, I. J.; McPartlin, M. *J. Am. Chem. Soc.* **1998**, *120*, 7239−7251.

10.1021/om700587w CCC: $37.00
Publication on Web 10/02/2007

Scheme 1

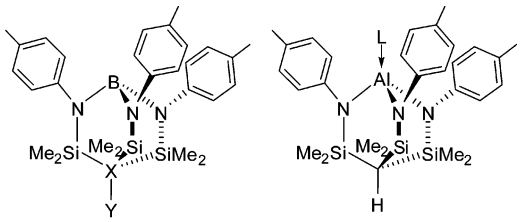

A (X = C, Y = H; X = Si, Y = Me) **B** (L = LiCl; THF)

Al complexes (e.g., structures **A** and **B** shown in Scheme 1) incorporating Gade's tripodal triamido $[N_3]^{3-}$ ligands[5] having the trisilylmethane or trisilylsilane backbone. A related ligand system is the *tetradentate* tripodal triamidoamine $N[N_3]^{3-}$ ligand; main-group (e.g., Verkade's boron and aluminum azatranes[6]) and transition-metal complexes bearing such a ligand have been extensively studied by Verkade[7] and Schrock.[8] Another related ligand system is the *tridentate* diamidoamine $N[N_2]^{2-}$ ligand, main-group B and Al complexes of which are also well-established.[9] On the other hand, to the best of our knowledge, B and Al complexes bearing the *tridentate* tripodal triamido $[N_3]^{3-}$ ligand were unknown prior to our recent report,[4a] and this ligand system has not been employed for the synthesis of relevant trivalent lanthanide (Ln) complexes, although its complexes with the yttrium center[10] and commonly the tetravalent metal centers including those of group 4 metals[11] are known. The tripodal triamido borane $[N_3]B$ can now be readily prepared, but the degree of pyramidalization in structure **A** is not remarkable.[4a] The synthetic routes to the analogous alane resulted in the formation of "$[N_3]Al$" as a salt (LiCl) or donor-solvent (tetrahydrofuran (THF)) adduct, implying a highly Lewis acidic Al center in $[N_3]Al$; however, the coordinated LiCl or THF in structure **B** cannot be removed via various methods. Hence, the *first goal* of the current work was to investigate various synthetic approaches that could potentially lead to isolation of the elusive salt- and solvent-free tripodal triamido Al and Ln complexes, $[N_3]Al$ and $[N_3]Ln$, with variations in the peripheral N-substituents and ligand backbone framework (including neopentane, trisilylmethane, and trisilylsilane backbones).

A wide range of organoaluminum and boron complexes have been extensively used as potent olefin polymerization activators[2] as well as efficient catalysts or initiators for ring-opening polymerization (ROP) of heterocyclic monomers[3] including lactides,[12] lactones,[13] and epoxides.[14] Thus, it is of interest to examine the reactivity and catalytic activity of the selected tripodal amido borane and alane complexes. Accordingly, our *second goal* of the current work was to investigate the abstractive chemistry of the tripodal borane pertinent to olefin polymerization catalysis as well as ROP of propylene oxide and ϵ-caprolactone (CL) by the tripodal alanes. For the CL polymerization, we emphasized the ROP of CL, employing an alcohol as chain-transfer reagent (CTR)[15] and a tripodal alane as catalyst for the *catalytic* production of biodegradable poly(ϵ-caprolactone).

Experimental Section

Materials and Methods. All syntheses and manipulations of air- and moisture-sensitive materials were carried out in flamed Schlenk-type glassware on a dual-manifold Schlenk line, on a high-vacuum line, or in an argon- or nitrogen-filled glovebox. HPLC grade organic solvents were sparged extensively with nitrogen during filling of the solvent reservoir and then dried by passage through activated alumina (for THF, Et_2O, and CH_2Cl_2) followed by passage through Q-5-supported copper catalyst (for toluene and hexanes) stainless steel columns. Benzene-d_6 and toluene-d_8 were degassed, dried over sodium/potassium alloy, and filtered before use, whereas $CDCl_3$ and CD_2Cl_2 were degassed and dried over activated Davison 4 Å molecular sieves. Propylene oxide and ϵ-caprolactone were degassed and dried over CaH_2 overnight and then vacuum-distilled before use. NMR spectra were recorded on a Varian Inova 300 (FT 300 MHz, ^{1}H; 96 MHz, ^{11}B; 75 MHz, ^{13}C) or a Varian Inova 400 spectrometer. Chemical shifts for ^{1}H

(5) For reviews, see: (a) Gade, L. H. *Acc. Chem. Res.* **2002**, *35*, 575−582. (b) Gade, L. H. *Chem. Commun. (Cambridge)* **2000**, 173−181. (c) Gade, L. H. *Angew. Chem., Int. Ed.* **2000**, *39*, 2658−2678.

(6) (a) Verkade, J. G. *Coord. Chem. Rev.* **1994**, *137*, 233−295. (b) Verkade, J. G. *Acc. Chem. Res.* **1993**, *26*, 483−489.

(7) (a) Duan, Z.; Naiini, A. A.; Lee, J.-H.; Verkade, J. G. *Inorg. Chem.* **1995**, *34*, 5477−5482. (b) Pinkas, J.; Wang, T.; Jacobson, R. A.; Verkade, J. G. *Inorg. Chem.* **1994**, *33*, 4202−4210. (c) Pinkas, J.; Gaul, B.; Verkade, J. G. *J. Am. Chem. Soc.* **1993**, *115*, 3925−3931.

(8) (a) Schrock, R. R. *Acc. Chem. Res.* **2005**, *38*, 955−962. (b) Schrock, R. R. *Acc. Chem. Res.* **1997**, *30*, 9−16.

(9) For selected examples, see: (a) Nelson, S. G.; Kim, B.-K.; Peelen, T. J. *J. Am. Chem. Soc.* **2000**, *122*, 9318−9319. (b) Emig, N.; Nguyen, H.; Krautscheid, H.; Réau, R.; Cazaux, J.-B.; Bertrand, G. *Organometallics* **1998**, *17*, 3599−3608. (c) Emig, N.; Réau, R.; Krautscheid, H.; Fenske, D.; Bertrand, G. *J. Am. Chem. Soc.* **1996**, *118*, 5822−5823.

(10) Memmler, H.; Walsh, K.; Gade, L. H. *Inorg. Chem.* **1995**, *34*, 4062−4068.

(11) (a) Turculet, L.; Tilley, T. D. *Organometallics* **2004**, *23*, 1542−1553. (b) Turculet, L.; Tilley, T. D. *Organometallics* **2002**, *21*, 3961−3972. (c) Jia, L.; Zhao, J.; Ding, E.; Brennessel, W. W. *J. Chem. Soc., Dalton Trans.* **2002**, 2608−2615. (d) Jia, L.; Ding, E.; Rheingold, A. L.; Rhatigan, B. *Organometallics* **2000**, *19*, 963−965.

(12) For selected recent examples, see: (a) Nomura, N.; Ishii, R.; Yamamoto, Y.; Kondo, T. *Chem. Eur. J.* **2007**, *13*, 4433−4451. (b) Du, H.; Pang, X.; Yu, H.; Zhuang, X.; Chen, X.; Cui, D.; Wang, X.; Jing, X. *Macromolecules* **2007**, *40*, 1904−1913. (c) Chisholm, M. H.; Patmore, N. J.; Zhou, Z. *Chem. Commun. (Cambridge)* **2005**, 127−129. (d) Hormnirun, P.; Marshall, E. L.; Gibson, V. C.; White, A. J. P.; Williams, D. J. *J. Am. Chem. Soc.* **2004**, *126*, 2688−2689. (e) Dechy-Cabaret, O.; Martin-Vaca, B.; Bourissou, D. *Chem. Rev.* **2004**, *104*, 6147−6176. (f) Zhong, Z.; Dijkstra, P.; Feijen, J. *J. Am. Chem. Soc.* **2003**, *125*, 11291−11298. (g) Nomura, N.; Ishii, R.; Akakura, M.; Aoi, K. *J. Am. Chem. Soc.* **2002**, *124*, 5938−5939. (h) Ovitt, T. M.; Lobkovsky, E. B.; Coates, G. W. *J. Am. Chem. Soc.* **2002**, *124*, 1316−1326. (i) O'Keefe, B. J.; Hillmyer, M. A.; Tolman, W. B. R. *J. Chem. Soc., Dalton Trans.* **2001**, 2215−2224. (j) Jhurry, D.; Bhaw-Luximon, A.; Spassky, N. *Macromol. Symp.* **2001**, *175*, 67−79. (k) Radano, C. R.; Baker, G. L.; Smith, M. R. *J. Am. Chem. Soc.* **2000**, *122*, 1552−1553.

(13) For selected recent examples, see: (a) Milione, S.; Grisi, F.; Centore, R.; Tuzi, A. *Organometallics* **2006**, *25*, 266−274. (b) Amgoune, A.; Lavanant, L.; Thomas, C. M.; Chi, Y.; Welter, R.; Dagorne, S.; Carpentier, J.-F. *Organometallics* **2005**, *24*, 6279−6282. (c) Lewiński, J.; Horeglad, P.; Tratkiewicz, E.; Grzenda, W.; Lipkowski, J.; Kolodziejczyk, E. *Macromol. Rapid Commun.* **2004**, *25*, 1939−1942. (d) Chen, C.-T.; Huang, C.-A.; Huang, B.-H. *Macromolecules* **2004**, *37*, 7968−7973. (e) Alcazar-Roman, L. M.; O'Keefe, B. J.; Hillmyer, M. A.; Tolman, W. B. *Dalton Trans.* **2003**, 3082−3087. (f) Liao, T.-C.; Huang, Y.-L.; Huang, B.-H.; Lin, C.-C. *Macromol. Chem. Phys.* **2003**, *204*, 885−892. (g) Chakraborty, D.; Chen, E. Y.-X. *Organometallics* **2003**, *22*, 769−774. (h) Chakraborty, D.; Chen, E. Y.-X. *Organometallics* **2002**, *21*, 1438−1442. (i) Hsueh, M.-L.; Huang, B.-H.; Lin, C.-C. *Macromolecules* **2002**, *35*, 5763−5768. (j) Yu, R.-C.; Hung, C.-H.; Huang, J.-H.; Lee, H.-Y.; Chen, J.-T. *Inorg. Chem.* **2002**, *41*, 6450−6455. (k) Liu, Y.-C.; Ko, B.-T.; Lin, C.-C. *Macromolecules* **2001**, *34*, 6196−6201.

(14) For selected recent examples, see: (a) Wasserman, E. P.; Annis, I.; Chopin, L. J., III; Price, P. C.; Petersen, J. L.; Abboud, K. A. *Macromolecules* **2005**, *38*, 322−333. (b) Chisholm, M. H.; Zhou, Z. *J. Am. Chem. Soc.* **2004**, *126*, 11030−11039. (c) Chakraborty, D.; Rodriguez, A.; Chen, E. Y.-X. *Macromolecules* **2003**, *36*, 5470−5481. (d) Braune W.; Okuda, J. *Angew. Chem., Int. Ed.* **2003**, *42*, 64−77468. (e) Chisholm, M. H.; Gallucci, J.; Phomphrai, K. *Inorg. Chem.* **2002**, *41*, 2785−2794. (f) Munoz-Hernandez, M.-A.; Mckee, M. L.; Keizer, T. S.; Yearwood, B. C.; Atwood, D. A. *J. Chem. Soc., Dalton Trans.* **2002**, 410−414. (g) Antelmann, B.; Chisholm, M. H.; Iyer, S.; Huffman, J. C.; Navarro-Llobet, D.; Pagel, M.; Simonsick, W. J.; Zhong, W. *Macromolecules* **2001**, *34*, 3159−3174.

(15) (a) Martin, E.; Dubois, P.; Jérôme, R. *Macromolecules* **2000**, *33*, 1530−1535. (b) Nomura, N.; Taira, A.; Tomioka, T.; Okada, M. *Macromolecules* **2000**, *33*, 1497−1499.

and ^{13}C spectra were referenced to internal solvent resonances and reported as parts per million relative to $SiMe_4$, while chemical shifts for ^{11}B spectra were referenced to external standard $BF_3 \cdot Et_2O$. IR spectra were recorded on a Nicolet Magna-760 FT/IR instrument. Elemental analyses were performed by Desert Analytics, Tucson, AZ. Unless otherwise specified, all commercial reagents were purchased from Aldrich Chemical Co. and used as received. Literature procedures were employed for the preparation of the following neutral tripodal amido ligands as well as Al, B, and Zr complexes: $HC[SiMe_2NHAr]_3$ (Ar = 4-MeC_6H_4, CH_2Ph),[16] $MeSi[SiMe_2NHAr]_3$ (Ar = 4-MeC_6H_4),[17] $MeC[CH_2NH(SiMe_3)]_3$,[18] AlH_3,[19] $Al[N(SiMe_3)_2]_3$,[20] $Sm[N(SiMe_3)_2]_3$,[21] $HC[SiMe_2NAr]_3B$ (Ar = 4-MeC_6H_4),[4a] Cp_2ZrMe_2,[22] and *rac*-$Et(Ind)_2ZrMe_2$.[23]

Synthesis of $HC[SiMe_2N(CH_2Ph)]_3Al\cdot(THF)$ (1). $HC[SiMe_2N(CH_2Ph)]_3Li_3(THF)_2$ was first isolated from the reaction of $HC[SiMe_2NH(CH_2Ph)]_3$ (0.61, 1.20 mmol) and ^{n}BuLi (2.25 mL, 1.6 M hexanes solution, 3.60 mmol) in Et_2O (30 mL) and THF (0.5 mL). This solid was dissolved in 10 mL of Et_2O and cooled to −30 °C, and to this solution was slowly added $AlCl_3$ (0.16 g, 1.20 mmol) in a solvent mixture (5 mL of hexanes and 10 mL of Et_2O). This mixture was warmed gradually to ambient temperature while being stirred for 14 h, after which the resulting mixture was filtered to remove LiCl precipitates. The filtrate was evaporated to dryness under vacuum, and the residue was extracted with hexanes (8 mL). The extract was kept at −30 °C for 3 days, affording 0.32 g (53% yield) of **1** as a colorless crystalline solid. ^1H NMR (C_6D_6, 23 °C): δ 7.66 (d, 6H), 7.28 (t, 6H), 7.09 (t, 3H) (CH_2Ph), 4.39 (s, 6H, CH_2Ph), 3.12 (br m, 4H, OCH_2CH_2), 0.52 (s, 18H, $SiMe_2$), 0.28 (br m, 4H, OCH_2CH_2), −0.36 (s, 1H, *H*C). Anal. Calcd for $C_{32}H_{48}AlN_3OSi_3$: C, 63.85; H, 8.04; N, 6.98. Found: C, 63.64; H, 7.78; N, 7.06.

Synthesis of $MeC[CH_2N(SiMe_3)]_3AlCl[Li(Et_2O)]$ (2). To a solution of $AlCl_3$ (0.133 g, 1.00 mmol) in a hexanes (10 mL)/Et_2O (10 mL) solvent mixture at −30 °C was added slowly a solution of $\{MeC[CH_2N(SiMe_3)]_3Li_3\}_2$ (0.35 g, 1.00 mmol) in a solvent mixture of hexanes (10 mL) and Et_2O (10 mL). The mixture was allowed to warm to room temperature and stirred for 12 h, after which it was filtered to remove LiCl precipitates. The filtrate was evaporated to dryness under vacuum, affording 0.27 g (57% yield) of **2** as a colorless crystalline solid. ^1H NMR (C_6D_6, 23 °C): δ 3.31 (s, 2H), 3.29 (d, 2H) (CH_2), 2.94 (q, 4H, OCH_2CH_3), 2.72 (d, 2H, CH_2), 0.84 (t, 6H, OCH_2CH_3), 0.57 (s, 3H, *Me*C), 0.49 (s, 9H, $SiMe_3$), 0.30 (s, 18H, $SiMe_3$). Anal. Calcd for $C_{18}H_{46}AlClLiN_3OSi_3$: C, 45.59; H, 9.78; N, 8.86. Found: C, 44.89; H, 9.78; N, 9.27.

Syntheses of $HC[SiMe_2NHAr][SiMe_2NAr]_2AlMe$ (Ar = 4-MeC_6H_4, 3; Ar = CH_2Ph, 4). To a solution of $HC[SiMe_2NH(4\text{-}MeC_6H_4)]_3$ (0.536 g, 1.06 mmol) in 30 mL of toluene at −30 °C was added $AlMe_3$ (0.53 mL, 2.0 M in hexanes, 1.06 mmol). The mixture was allowed to warm gradually to ambient temperature while being stirred for 12 h, after which the resulting solution was slowly heated to reflux for 4 h. The solution was cooled to ambient temperature and evaporated to dryness under vacuum. The residue was extracted with hexanes (5 mL), and the hexanes extract was kept at −30 °C for ca. 2 months, affording 0.15 g (25%) of **3** as an off-white solid. ^1H NMR (C_6D_6, 23 °C): δ 7.23 (d, 4H), 7.11 (d, 4H), 6.68 (br, 4H) (4-MeC_6H_4), 3.85 (s, 1H, N*H*), 2.21 (s, 6H), 1.93 (s, 3H) (4-*Me*C_6H_4), 0.45 (br, 12H), 0.21 (br, 6H) ($SiMe_2$), −0.69 (s, 3H, Al*Me*), −0.76 (s, 1H, *H*C). Complex **4** was synthesized in a manner similar to that of **3**. $AlMe_3$ (0.55 mL, 2.0 M in hexanes, 1.10 mmol), $HC[SiMe_2NH(CH_2Ph)]_3$ (0.56 g, 1.10 mmol), and toluene (30 mL) were used, producing 0.50 g (83% yield) of **4** as a colorless crystalline solid. ^1H NMR (C_6D_6, 23 °C): δ 7.53 (d), 7.32 (t), 7.18 (br), 6.98−7.02 (br m), 6.78−6.83 (br m) (15H, CH_2Ph), 4.25−4.32 (m, 4H), 3.52−3.82 (m, 2H) (CH_2Ph), 1.95 (dd, 1H, N*H*), 0.25 (s), 0.18 (s), 0.03 (br) (18H, $SiMe_2$), −0.54 (s, 3H, Al*Me*), −0.95 (s, 1H, *H*C). Selected VT ^1H NMR data in C_7D_8 were listed as follows: −70 °C, δ 7.65 (d), 7.42 (t), 7.40 (t), 7.23 (t), 6.88−7.10 (m), 6.80−6.82 (br m), 6.35 (d) (15H, CH_2Ph), 4.53 (d), 4.48 (d), 4.33 (d), 4.28 (d) (4H, CH_2Ph), 3.68 (dd), 3.30 (dd) (2H, CH_2Ph), 1.95 (dd, 1H, N*H*), 0.29 (s, 3H), 0.27 (s, 3H), 0.22 (s, 3H), 0.20 (s, 3H), 0.10 (s, 3H), −0.29 (s, 3H) ($SiMe_2$), −0.42 (s, 3H, Al*Me*), −1.29 (s, 1H, *H*C); 20 °C, δ 7.46 (d), 7.27 (t), 6.90−7.15 (m), 6. 86 (br) (15H, CH_2Ph), 4.17−4.31 (m) (4H, CH_2Ph), 3.50−3.80 (m, 2H, CH_2Ph), 1.94 (dd, 1H, N*H*), 0.17 (br s), 0.13 (br), −0.09 (br) (18H, $SiMe_2$), −0.60 (s, 3H, Al*Me*), −0.97 (s, 1H, *H*C); 60 °C, δ 7.43 (br), 7.22 (br), 6.80−7.20 (br m), (15H, CH_2Ph), 4.21 (br, 4H, CH_2Ph), 3.68 (br m, 2H, CH_2Ph), 1.96 (br, 1H, N*H*), 0.14 (br, 18H) ($SiMe_2$), −0.66 (s, 3H, Al*Me*), −0.90 (s, 1H, *H*C). $^{13}C\{^1H\}$ (C_6D_6, 23 °C): δ 147.2, 138.1, 127.6, 126.9, 126.1 (CH_2Ph), 49.5, 47.4 (CH_2Ph), 6.9 (H*C*), 4.52 (br), 2.88 (br) ($SiMe_2$), −14.3 (br, Al*Me*). Anal. Calcd for $C_{29}H_{44}AlN_3Si_3$: C, 63.80; H, 8.12; N, 7.70. Found: C, 63.42; H, 8.16; N, 7.53.

Synthesis of $[(4\text{-}MeC_6H_4)HNMe_2Si](H)C[SiMe_2N(4\text{-}MeC_6H_4)]_2(AlMe_2)_2$ (5). To a solution of $HC[SiMe_2NH(4\text{-}MeC_6H_4)]_3$ (0.254 g, 0.50 mmol) in 30 mL of toluene at −30 °C was added $AlMe_3$ (1.60 mL, 1.0 M in toluene, 1.60 mmol). The resulting mixture was allowed to warm gradually to ambient temperature while being stirred for 20 h. The obtained solution was evaporated to dryness under vacuum, and the residue was washed with hexanes (2 × 1 mL) to give, after drying in vacuo, 0.18 g (59%) of **5** as an off-white solid. ^1H NMR (C_6D_6, 23 °C): δ 6.84−6.98 (m, 6H), 6.85 (d, 4H), 6.53 (d, 2H) (4-MeC_6H_4), 3.10 (s, 1H, N*H*), 2.12 (s, 3H), 2.02 (s, 6H) (4-*Me*C_6H_4), 1.11 (s, 1H, *H*C), 0.45 (s, 6H), 0.36 (s, 6H), 0.26 (s, 6H) ($SiMe_2$), 0.21 (s, 3H), 0.18 (s, 3H), −0.52 (s, 6H) ($AlMe_2$). Anal. Calcd for $C_{32}H_{53}Al_2N_3Si_3$: C, 62.19; H, 8.64; N, 6.80. Found: C, 61.73; H, 8.42; N, 6.24.

Synthesis of $[(Me_3Si)HNCH_2](Me)C[CH_2N(SiMe_3)]_2(AlMe_2)_2$ (6). To a solution of $MeC[CH_2NH(SiMe_3)]_3$ (0.67 g, 2.00 mmol) in 30 mL of toluene at ambient temperature was added $AlMe_3$ (1.0 mL, 2.0 mmol, 2.0 M in toluene). The mixture was stirred at this temperature for 2 h and then subjected to reflux for 12 h. After being cooled to room temperature, the resulting solution was evaporated to dryness under vacuum, affording an oily mixture (by ^1H NMR). To this oil was added toluene (20 mL) and $AlMe_3$ (2.0 mL, 4.0 mmol, 2.0 M in toluene). The mixture was stirred for 24 h, after which all volatiles were removed under vacuum and the residue was extracted into hexanes (3 mL). The extract was kept at −30 °C for 2 days, affording 0.32 g (36%) of **6** as colorless crystals. ^1H NMR (C_6D_6, 23 °C): δ 2.48−3.36 (m, 6H, CH_2), 1.09 (t, 1H, N*H*), 0.18 (s, 3H, *Me*C), 0.12 (s, 12H, $SiMe_3$, Al*Me*), −0.10 (s, 9H), −0.27 (s, 9H) ($SiMe_3$), −0.15 (s, 3H), −0.40 (s, 3H), −0.59 (s, 3H) (Al*Me*). $^{13}C\{^1H\}$ (C_6D_6, 23 °C): δ 57.8, 57.2, 54.9 (CH_2), 34.5 (Me*C*), 23.8 (*Me*C), −0.01, −0.5, −0.8 ($SiMe_3$), −3.8 (br), −6.9 (br), −10.1 (br) (Al*Me*). Anal. Calcd for $C_{18}H_{49}Al_2N_3Si_3$: C, 48.49; H, 11.08; N, 9.43. Found: C, 48.10; H, 11.08; N, 9.21.

(16) Memmler, H.; Gade, L. H.; Lauher, J. W. *Inorg. Chem.* **1994**, *33*, 3064−3071.

(17) Schubart, M.; Findeis, B.; Gade, L. H.; Li, W.-S.; McPartlin, M. *Chem. Ber.* **1995**, *128*, 329−334.

(18) Gade, L. H.; Mahr, N. *J. Chem. Soc., Dalton Trans.* **1993**, 489−494.

(19) (a) Brower, F.; Matzek, N. E.; Reigler, P. F.; Rinn, H. W.; Roberts, C. B.; Schmidt, D. L.; Snover, J. A.; Terada, K. *J. Am. Chem. Soc.* **1976**, *98*, 2450−2453. (b) Yartys, V. A.; Denys, R. V.; Maehlen, J. P.; Frommen, C.; Fichtner, M.; Bulychev, B. M.; Emerich, H. *Inorg. Chem.* **2007**, *46*, 1051−1055.

(20) Paciorek, K. J. L.; Nakahara, J. H.; Masuda, S. R. *Inorg. Chem.* **1990**, *29*, 4252−4255.

(21) Schueta, S.; Day, V. W.; Sommer, R. D.; Rheingold, A. L.; Belot, J. A. *Inorg. Chem.* **2001**, *40*, 5292−5295.

(22) Samuel, E.; Rausch, M. D. *J. Am. Chem. Soc.* **1973**, *95*, 6263−6267.

(23) Diamond, G. M.; Jordan, R. F.; Petersen, J. L. *J. Am. Chem. Soc.* **1996**, *118*, 8024−8033.

Synthesis of [{HC[SiMe$_2$N(4-MeC$_6$H$_4$)]$_3$AlH}Li]$_2$ (7) and 7·(OEt$_2$)$_2$. Precooled toluene (20 mL) was added to a mixture of HC[SiMe$_2$NH(4-MeC$_6$H$_4$)]$_3$ (0.25 g, 0.50 mmol) and LiAlH$_4$ (0.08 g, 2.10 mmol). The resulting suspension was stirred at ambient temperature for 36 h, after which it was filtered and the filtrate was evaporated to dryness under vacuum. The residue was extracted with hexanes (2 mL), and the extract was kept at −30 °C for 3 days, affording 0.10 g (37%) of **7** as a colorless crystalline solid. ^{1}H NMR (C$_6$D$_6$, 23 °C): δ 7.02 (q$_{AB}$, 12H), (4-MeC$_6$*H*$_4$), 2.18 (s, 9H, 4-*Me*C$_6$H$_4$), 0.26 (s, 18H, Si*Me*$_2$), −0.77 (s, 1H, *H*C). Mixing of this compound with Et$_2$O afforded its ether adduct **7**·(Et$_2$O)$_2$. ^{1}H NMR (C$_6$D$_6$, 23 °C): δ 7.24 (d, 6H), 7.00 (d, 6H) (4-MeC$_6$*H*$_4$), 3.03 (q, 8H, OC*H*$_2$CH$_3$), 2.18 (s, 9H, 4-*Me*C$_6$H$_4$), 0.84 (t, 12H, OCH$_2$C*H*$_3$), 0.44 (s, 18H, Si*Me*$_2$), −0.57 (s, 1H, *H*C). IR (NaCl plate, Nujol mull, cm^{-1}): ν 1807 (w, AlH). Anal. Calcd for C$_{36}$H$_{61}$AlLiN$_3$O$_2$Si$_3$: C, 63.02; H, 8.96; N, 6.12. Found: C, 62.64; H, 8.62; N, 6.13.

Synthesis of MeSi[SiMe$_2$N(4-MeC$_6$H$_4$)]$_3$AlH(AlH$_2$) (8). Toluene (30 mL) was added to a mixture of MeSi[SiMe$_2$NH(4-MeC$_6$H$_4$)]$_3$ (0.36 g, 0.67 mmol) and AlH$_3$ (0.02 g, 0.67 mmol) at ambient temperature. The resulting suspension was stirred at this temperature for 0.5 h and then heated to reflux for 3 h. After being cooled to ambient temperature, all volatiles of the reaction mixture were removed under vacuum to give a viscous oil. This oil was dissolved in toluene (10 mL) and was added to a second portion of AlH$_3$ (0.04 g, 1.33 mmol). The mixture was stirred overnight and then filtered; the filtrate was evaporated to dryness under vacuum, and the residue was extracted with hexanes (5 mL). The extract was kept at −30 °C for 24 h to produce 0.20 g (53% based on the neutral ligand) of **8** as a crystalline solid. ^{1}H NMR (C$_6$D$_6$, 23 °C): δ 6.75−7.26 (m, 8H), 6.77 (d, 4H) (4-MeC$_6$*H*$_4$), 2.23 (s, 3H), 1.94 (s, 6H) (4-*Me*C$_6$H$_4$), 0.77 (s, 6H), 0.44 (6H), 0.27 (s, 6H) (Si*Me*$_2$), 0.13 (s, 3H, *Me*Si). IR (NaCl plate, Nujol mull, cm^{-1}): ν 1873 (s), 1844 (s) (AlH). Anal. Calcd for C$_{28}$H$_{45}$Al$_2$N$_3$Si$_4$: C, 57.00; H, 7.69; N, 7.12. Found: C, 57.17; H, 7.53; N, 6.90.

Synthesis of {MeSi[SiMe$_2$N(4-MeC$_6$H$_4$)]$_3$Sm}$_2$ (9). A solution of Sm[N(SiMe$_3$)$_2$]$_3$ (0.107 g, 0.167 mmol) and MeSi[SiMe$_2$NH(4-MeC$_6$H$_4$)]$_3$ (0.09 g, 0.167 mmol) in toluene (40 mL) was stirred for 2 h at room temperature and then subjected to reflux for 12 h. After being cooled to room temperature, the solution was evaporated to dryness under vacuum. The residue was washed with hexanes to afford 0.062 g (77%) of **9** as a light yellow solid. ^{1}H NMR (C$_6$D$_6$, 23 °C): δ 11.7 (br, 6H), 6.13 (br, 6H) (4-MeC$_6$*H*$_4$), 1.16 (br, 9H, 4-*Me*C$_6$H$_4$), 0.31 (br, 18H, Si*Me*$_2$), −3.50 (s, 3H, *Me*Si). Anal. Calcd for C$_{56}$H$_{84}$N$_6$Si$_6$Sm$_2$: C, 49.21; H, 6.19; N, 6.15. Found: C, 48.63; H, 6.13; N, 5.79.

Reaction of HC[SiMe$_2$N(4-MeC$_6$H$_4$)]$_3$B with AlMe$_3$ and Isolation of HC[SiMe$_2$N(4-MeC$_6$H$_4$)]$_3$BMe(AlMe$_2$) (10). To a solution of HC[SiMe$_2$N(4-MeC$_6$H$_4$)]$_3$B (51.3 mg, 0.10 mmol) in toluene (10 mL) at −30 °C was added AlMe$_3$ (4.8 μL, 0.10 mmol). The mixture was stirred for 6 h, during which time it was freely warmed to ambient temperature. The obtained solution was evaporated to dryness, and the residue was extracted into hexanes (5 mL). The hexanes extract was concentrated to ca. 1 mL and kept at −30 °C for 4 days, affording 41.0 mg (70%) of **10** as colorless crystals. ^{1}H NMR (C$_6$D$_6$, 23 °C): δ 6.86−7.00 (m, 10H), 6.70 (d, 2H) (4-MeC$_6$*H*$_4$), 2.11 (s, 3H), 2.05 (s, 6H) (4-*Me*C$_6$H$_4$), 1.66 (s, 1H, *H*C), 0.46 (s, 6H), 0.44 (s, 6H) (Si*Me*$_2$), 0.35 (s, 3H, B*Me*), 0.29 (s, 3H), 0.08 (s, 3H) (Si*Me*$_2$), −0.49 (s, 3H), −0.53 (s, 3H) (Al*Me*$_2$). ^{11}B (C$_6$D$_6$, 23 °C): δ 37.5 (br). Anal. Calcd for C$_{31}$H$_{49}$AlBN$_3$Si$_3$: C, 63.56; H, 8.43; N, 7.17. Found: C, 63.08; H, 8.25; N, 6.61.

Reaction of HC[SiMe$_2$N(4-MeC$_6$H$_4$)]$_3$B with AlH$_3$ and Isolation of HC[SiMe$_2$N(4-MeC$_6$H$_4$)]$_3$AlH(BH$_2$) (11). The mixture of HC[SiMe$_2$N(4-MeC$_6$H$_4$)]$_3$B (51.5 mg, 0.10 mmol) and AlH$_3$ (3.0 mg, 0.10 mmol) in toluene (5 mL) was stirred for 3 h at ambient temperature, after which all volatiles were removed under vacuum. The resulting residue was extracted into hexanes (5 mL), and the extract was kept at −30 °C overnight to give 46.0 mg (84%) of **11** as a crystalline solid. ^{1}H NMR (C$_6$D$_6$, 23 °C): δ 7.15−7.34 (m, 8H), 6.83 (d, 4H) (4-MeC$_6$*H*$_4$), 2.22 (s, 3H), 1.99 (s, 6H) (4-*Me*C$_6$H$_4$), 0.52 (s, 6H), 0.33 (s, 6H), 0.19 (s, 6H) (Si*Me*$_2$), −0.93 (s, 1H, *H*C). ^{11}B (C$_6$D$_6$, 23 °C): δ −6.23 (br). IR (NaCl plate, Nujol mull, cm^{-1}): ν 2401 (w), 2361 (w) (BH), 1900 (w, AlH). Anal. Calcd for C$_{28}$H$_{43}$AlBN$_3$Si$_3$: C, 61.85; H, 7.97; N, 7.73. Found: C, 61.73; H, 7.26; N, 7.18.

Reaction of HC[SiMe$_2$N(4-MeC$_6$H$_4$)]$_3$B with Cp$_2$ZrMe$_2$ and Isolation of Cp$_2$ZrMe[N(4-MeC$_6$H$_4$)SiMe$_2$](H)C[SiMe$_2$N(4-MeC$_6$H$_4$)]$_2$BMe (12). In an argon-filled glovebox, a 30 mL glass reactor was equipped with a stir bar and charged with Cp$_2$ZrMe$_2$ (50.3 mg, 0.20 mmol), HC[SiMe$_2$N(4-MeC$_6$H$_4$)]$_3$B (103 mg, 0.20 mmol), and toluene (5 mL) at ambient temperature. The mixture was stirred for 10 min to give a light yellow solution. The solution was evaporated to dryness under vacuum, and the residue was extracted with hexanes and filtered. The filtrate was evaporated to dryness, affording 146 mg (95%) of **12** as a light yellow solid. ^{1}H NMR (C$_6$D$_6$, 23 °C): δ 6.87−6.97 (m, 10H), 6.68 (d, 2H) (4-MeC$_6$*H*$_4$), 5.68 (s, 10H, Cp*H*), 2.18 (s, 3H), 2.13 (s, 6H) (4-*Me*C$_6$H$_4$), 0.50 (br, 7H, *H*C, Si*Me*$_2$), 0.44 (s, 6H, Si*Me*$_2$), 0.31 (s, 3H, B*Me*), 0.25 (s, 6H, Si*Me*$_2$), 0.05 (s, 3H, Zr*Me*). ^{11}B NMR (C$_6$D$_6$, 23 °C): δ 35.0 (br). Anal. Calcd for C$_{40}$H$_{56}$BN$_3$Si$_3$Zr: C, 62.78; H, 7.38; N, 5.49. Found: C, 62.36; H, 7.06; N, 5.76.

Reaction of HC[SiMe$_2$N(4-MeC$_6$H$_4$)]$_3$B with *rac*-Et(Ind)$_2$ZrMe$_2$ and Isolation of *rac*-Et(Ind)$_2$ZrMe[N(4-MeC$_6$H$_4$)SiMe$_2$](H)C-[SiMe$_2$N(4-MeC$_6$H$_4$)]$_2$BMe (13). Isolation of **13** was carried out in the same manner as that of **12**. *rac*-Et(Ind)$_2$ZrMe$_2$ (75.5 mg, 0.20 mmol), HC[SiMe$_2$N(4-MeC$_6$H$_4$)]$_3$B (103 mg, 0.20 mmol), and toluene (5 mL) were used to produce 169 mg (95%) of **13** as a light yellow solid. ^{1}H NMR (C$_6$D$_6$, 23 °C): δ 7.56 (dd, 2H), 7.33 (d, 1H), 6.87−7.14 (m, 17H) (C$_6$*H*$_4$), 6.19 (d, 1H), 5.70 (d, 1H), 5.63 (d, 1H), 5.60 (d, 1H) (C$_5$*H*$_2$), 2.99 (m, 1H), 2.85 (m, 3H) (C*H*$_2$C*H*$_2$), 2.13 (s, 3H), 2.11 (s, 6H) (4-*Me*C$_6$H$_4$), 0.56 (s, 1H, *H*C), 0.48 (s, 3H), 0.43 (s, 3H), 0.42 (s, 3H), 0.20 (s, 6H), 0.07 (s, 3H) (Si*Me*$_2$), 0.21 (s, 3H, B*Me*), −0.67 (s, 3H, Zr*Me*). ^{11}B NMR (C$_6$D$_6$, 23 °C): δ 37.1 (br). Anal. Calcd for C$_{50}$H$_{62}$BN$_3$Si$_3$Zr: C, 67.37; H, 7.01; N, 4.71. Found: C, 67.05; H, 7.35; N, 4.43.

Polymerization Procedures. Polymerizations of propylene oxide (PO) and CL were carried out in a Schlenk line and in an argon-filled glovebox, respectively, following literature procedures.[13f,g,14c] In a typical experiment, 22.5 μmol of the tripodal amido aluminum catalyst was dissolved in 1 mL of CH$_2$Cl$_2$ and then added to CL (0.50 mL, [CL]/[cat.] = 200) with or without BnOH in 4 mL of CH$_2$Cl$_2$. The solution was stirred at ambient temperature. After a measured time interval, the reactor was taken out of the box, and methylene chloride was added to dissolve the polymer gel. The solution was precipitated into cold methanol (50 mL), filtered, washed with methanol, and dried in a vacuum oven at 50 °C overnight to a constant weight.

Gel permeation chromatography (GPC) analyses of the polymers were carried out at 40 °C and a flow rate of 1.0 mL/min, with CHCl$_3$ as the eluent, on a Waters University 1500 GPC instrument equipped with four 5 μm PL gel columns (Polymer Laboratories) and calibrated using 10 poly(methyl methacrylate) (PMMA) standards. Chromatograms were processed with Waters Empower software (version 2002); number-average molecular weight and polydispersity of polymers were given relative to PMMA standards.

X-ray Crystallographic Analyses of Complexes 2, 4, 5, 8, 9, and 13·1.2(Hexanes). Single crystals of all complexes suitable for X-ray diffraction were grown from hexanes or hexanes/toluene mixture at −30 °C inside the freezer of a glovebox. The crystals were quickly covered with a layer of Paratone-N oil (Exxon, dried and degassed at 120 °C/10^{-6} Torr for 24 h) after the mother liquors were decanted and then mounted on a thin glass fiber and transferred into the cold nitrogen stream of a Bruker SMART CCD diffrac-

Table 1. Crystal Data and Structure Refinements for 2, 4, 5, 8, 9, and 13·1.2(Hexanes)[a]

	compd **2**	compd **4**	compd **5**	compd **8**	compd **9**	compd **13**·1.2(hexanes)
formula	$C_{18}H_{46}AlClLiN_3OSi_3$	$C_{29}H_{44}AlN_3Si_3$	$C_{32}H_{53}Al_2N_3Si_3$	$C_{28}H_{45}Al_2N_3Si_4$	$C_{56}H_{84}N_6Si_8Sm_2$	$C_{57.20}H_{78.80}BN_3Si_3Zr$
Fw	474.22	545.92	618.00	589.99	1366.71	994.73
cryst syst	monoclinic	triclinic	orthorhombic	monoclinic	triclinic	monoclinic
space group	$P2_1/n$	$P\bar{1}$	$Pca2_1$	$C2/c$	$P\bar{1}$	$C2/c$
a/Å	11.5500(2)	9.8773(3)	39.9056(13)	36.5620(30)	13.9744(6)	43.7510(12)
b/Å	16.0631(3)	11.8618(4)	9.3888(3)	9.5547(9)	14.4704(6)	12.7618(4)
c/Å	15.9430(3)	13.7028(5)	19.4839(9)	19.4147(16)	18.2232(8)	26.9246(7)
α/deg		105.722(2)			84.707(3)	
β/deg	92.407(1)	93.966(2)		100.698(6)	80.305(3)	127.374(2)
γ/deg		96.701(2)			63.979(2)	
V/Å^3	2955.3(1)	1526.3(1)	7299.9(5)	6664.4(10)	3263.5(2)	11946.7(6)
Z	4	2	8[b]	8	2	8
ρ_{calcd}/(g·cm^{-3})	1.066	1.188	1.125	1.176	1.391	1.106
μ/mm^{-1}	0.293	0.207	0.203	0.253	1.967	0.279
F(000)	1032	588	2672	2528	1396	4240
cryst size/mm^3	0.41 0.32 0.09	0.35 0.12 0.08	0.20 0.18 0.05	0.24 0.18 0.06	0.39 0.08 0.06	0.22 0.16 0.07
θ range/deg	1.80−32.58	1.55−30.53	1.46−28.26	2.21−33.39	1.64−33.19	1.17−28.28
index ranges	$-16 \le h \le 17$	$-14 \le h \le 14$	$-53 \le h \le 53$	$-56 \le h \le 55$	$-21 \le h \le 21$	$-57 \le h \le 58$
	$-24 \le k \le 24$	$-16 \le k \le 16$	$-12 \le k \le 12$	$-14 \le k \le 12$	$-22 \le k \le 22$	$-17 \le k \le 17$
	$-23 \le l \le 24$	$-19 \le l \le 19$	$-24 \le l \le 25$	$-29 \le l \le 29$	$-24 \le l \le 28$	$-35 \le l \le 35$
collecd data	36 805	44 963	78 291	54 156	71 422	175 125
unique data (R_{int})	10 684 (0.0421)	9 305 (0.0510)	17 704 (0.0873)	12 328 (0.1652)	24 333 (0.0775)	14 811 (0.1306)
completeness to θ/%	99.3	99.6	99.7	95.1	97.3	99.9
data/restraints/params	10684/62/313	9305/0/336	17704/1/747	12328/0/356	24333/0/664	14811/20/632
GOF on F^2	0.994	1.015	0.997	1.052	1.086	1.022
final R indices [$I > 2\sigma(I)$]						
R_1	0.0446	0.0394	0.0508	0.1117	0.1160	0.0699
R_{w2}	0.1052	0.0893	0.0984	0.2386	0.2877	0.1794
R indices (all data)						
R_1	0.0765	0.0607	0.0837	0.2428	0.1563	0.1212
R_{w2}	0.1209	0.0990	0.1113	0.2942	0.3050	0.2172

[a] All data were collected at 173(2) K using Mo Kα ($\lambda = 0.710\,73$ Å) radiation. $R_1 = \Sigma(||F_o| - |F_c||)/\Sigma|F_o|$, $R_{w2} = \{\Sigma[w(F_o^2 - F_c^2)^2/\Sigma[w(F_o^2)^2]\}^{2}\}^{1/2}$, GOF $= \{\Sigma[w(F_o^2 - F_c^2)^2]/(N_o - N_p)\}^{1/2}$. [b] There were two solved independent molecules.

tometer. The structures were solved by direct methods and refined using the Bruker SHELXTL program library by full-matrix least-squares on F^2 for all reflections.[24] Unless otherwise indicated, all non-hydrogen atoms were located by difference Fourier synthesis and refined with anisotropic displacement parameters, whereas hydrogen atoms were included in the structure factor calculations at idealized positions. In **2**, the coordinated Et_2O solvent molecule at Li atom was disordered and treated in part (O(1)C(6)C(7)C(8)-C(9), 36%; O(1A)C(6A)C(7A)C(8A)C(9A), 64%). Due to the significant vibration of these two groups which resulted in the refining instability of atom positions, the suitable restriction was employed, giving 62 least-squares restraints and one of carbon atoms larger U_{eq} [C(7a), 0.166(4)Å^2]. In **4** and **8**, the NH and AlH hydrogen atoms were located by difference Fourier synthesis but refined isotropically. In **5**, two independent molecules were disclosed. In **9**, C(53) was refined isotropically due to the nonpositivity when treated aniostropically. The weak intensity X-ray diffraction data of **8** and **9** resulted from the crystal quality. Although the X-ray data of the two complexes was not of high quality, the data led to reasonable structural determinations, allowing for a brief discussion on their metric parameters. In **13**·1.2(hexanes), the hexanes solvent molecules were disordered and treated in part (C(71A)C(72A)C(73A)C(74A)C(75A)C(76A), 33%; C(71B)-C(72B)C(73B)C(74B)C(75B)C(76B), 27%; C(81A)C(82A)C(83A)-C(84A)C(85A)C(86A), 30%; C(81B)C(82B)C(83B)C(84B)C(85B)-C(86B), 30%), in which the carbon atoms were refined isotropically. Selected crystal data and structural refinement parameters are collected in Table 1.

Results and Discussion

Salt Metathesis Route. We previously reported the synthesis of tripodal triamido alane structure **B** via salt metathesis between tripodal triamido lithium salt $HC[SiMe_2N(4\text{-}MeC_6H_4)]_3Li_3$ and $AlCl_3$.[4a] Variations of the reaction medium (hexanes/toluene, Et_2O, or THF) gave rise to the formation of diverse adducts of the transient $[N_3]Al$ with THF, LiCl, $ClLi(Et_2O)_2$, and $Li(OCH{=}CH_2)(THF)_2$; the salt- or solvent-free $[N_3]Al$ cannot be isolated from these adducts via a variety of methods. We reasoned that two approaches could potentially solve this problem: the first is to employ the *N*-benzyl substituent for providing stabilization of the highly Lewis acidic Al center in $[N_3]Al$ via the proposed η^6-arene coordination of the benzyl group to Al, which could facilitate the removal of the coordinated donor solvent or salt. The second approach is to adjust the binding pocket size for Al by changing the tripodal ligand backbone framework.

For the first approach, we carried out the reaction of $HC[SiMe_2N(CH_2Ph)]_3Li_3(THF)_2$ with $AlCl_3$, which led to the corresponding tripodal triamido alane **1** as a THF adduct in 53% yield (Scheme 2). The ^{1}H NMR spectrum of **1** in C_6D_6 at room temperature exhibits only one set of aromatic resonances, a single benzyl−methylene peak, and a single $SiMe_2$−methyl peak, consistent with an apparent 3-fold symmetry in solution. The resonances for the coordinated THF protons were observed at 3.12 (m) and 0.28 (m) ppm. However, as in the case of the *N*-4-MeC_6H_4 substituted derivative **B** (L = THF), the coordinated THF in **1** was not removed upon heating under high-vacuum conditions.

For the second approach, we employed the tripodal triamido ligand having the neopentane backbone. Accordingly, the reaction of $\{MeC[CH_2N(SiMe_3)]_3Li_3\}_2$[18] with $AlCl_3$ in a Et_2O/hexanes solvent mixture gave an incomplete LiCl-elimination product (**2**, Scheme 3), which was isolated as a crystalline solid in 57% yield. This observation seems to reflect the donor solvent effect (Et_2O vs THF) more than the ligand framework effect on the formation of different salt-metathesis products, as we

(24) *SHELXTL*, Version 6.12; Bruker Analytical X-ray Solutions: Madison, WI, 2001.

Scheme 2

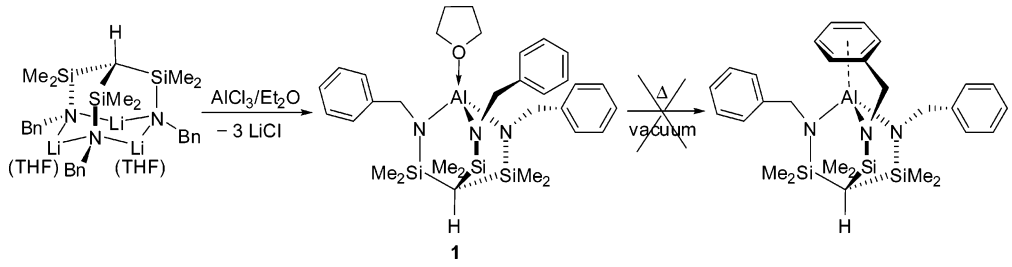

1

Scheme 3

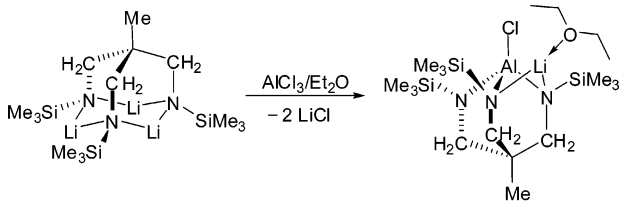

2

previously observed the similar product, HC[Si(Me$_2$)N(4-MeC$_6$H$_4$)]$_3$Al·ClLi(Et$_2$O)$_2$,[4a] from the reaction using a different ligand framework with the trisilyl methane backbone but the same solvent (i.e., no THF in the reaction medium or without the use of the preformed THF-solvated lithium salt).

The ^{1}H NMR spectrum of **2** exhibits three sets of resonances for the backbone methylene protons [3.31 (s, 2H), 3.29 (d, 2H), and 2.70 (d, 2H) ppm] and two sets of resonances for the SiMe$_3$ methyl protons [0.48 (s, 9H) and 0.30 (s, 18H) ppm], showing a non-3-fold symmetry in solution. This NMR feature is in sharp contrast to HC[SiMe$_2$N(4-MeC$_6$H$_4$)]$_3$Al·ClLi(Et$_2$O)$_2$,[4a] which presents a 3-fold symmetric ^{1}H NMR feature because the ether-solvated Li is coordinated to the terminal Cl, not to amido nitrogen atoms as in **2**. The molecular structure of **2** was determined by X-ray single-crystal diffraction analysis (Figure 1), confirming the solution structure derived from the NMR analysis. The remaining Al−Cl and three newly formed Al−N bonds render the Al center to a distorted tetrahedral geometry.

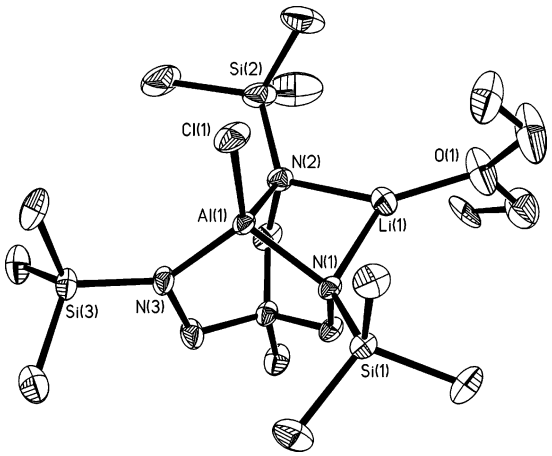

Figure 1. X-ray crystal structure of **2** with thermal ellipsoids drawn at the 50% probability and the disordered Et$_2$O of 36% occupancy. Selected bond lengths (Å) and angles (deg): Al−Cl(1), 2.143(1); Al−N(1), 1.870(1); Al−N(2), 1.881(1); Al−N(3), 1.803(1); Li(1)−N(1), 2.049(3); Li(1)−N(2), 2.057(3); Li(1)−O(1), 1.891-(11); N(1)−Al(1)−N(2), 94.1(1); N(1)−Al(1)−N(3), 108.4(1); N(2)−Al(1)−N(3), 108.4(1); Cl(1)−Al(1)−N(1), 112.5(1); Cl(1)−Al(1)−N(2), 111.6(1); Cl(1)−Al(1)−N(3), 119.0(1); N(1)−Li(1)−N(2), 83.9(1); N(1)−Li(1)−O(1), 138.6(4); N(2)−Li(1)−O(1), 136.3(4).

The Al−Cl bond length in **2** [2.143(1) Å] is considerably shorter than that in the dimeric {HC[SiMe$_2$N(4-MeC$_6$H$_4$)]$_3$Al·ClLi}$_2$ [2.227(1) Å] in which the Cl atom is also involved in the Cl$_2$Li$_2$ ring coordination,[4a] but it compares well to the four-coordinate terminal Al−Cl bond length of 2.153(1) Å found in HC[(CMe)(NAr)]$_2$AlClI (Ar = 2,6-^{i}Pr$_2$C$_6$H$_3$).[25] The Li atom keeps its original side coordination between two amido N atoms[18] and further links to one Et$_2$O solvent molecule, forming a triangular geometry ($\Delta_{Li(1)N(1)N(2)O(1)}$ = 0.0422 Å) with the Li−N bond distances of 2.049(3) and 2.057(3) Å as well as the Li−O distance of 1.890(8) (av) Å. This bonding motif gives rise to three nonequivalent tripodal arms and thus variations in Al−N bond lengths [1.803(1); 1.870(1) and 1.881(1) Å] and in N−Al−N angles [94.1(1); 108.4(1) and 108.4(1)°]. Similar structural features have been observed in group 14 tripodal triamido lithium adducts.[26]

Ligand Elimination Route. Verkade[7] and Gade[27] have shown that reactions of the neutral tetradentate tripodal tris(2-aminoethyl)amine ligand N[N$_3$]H$_3$ with AlR$_3$ (R = Me, NMe$_2$) readily generate the corresponding complete alkane or amine elimination products—aluminum azatranes. On the other hand, we found that reactions between the tridentate tripodal triamine ligand [N$_3$]H$_3$ and AlMe$_3$ show complexity.[28] Monitoring of the reaction between HC[SiMe$_2$NH(4-MeC$_6$H$_4$)]$_3$ and 1 equiv of AlMe$_3$ in C$_6$D$_6$ by ^{1}H NMR revealed several N*H* resonances from 4.00 to 3.00 ppm, indicative of the formation of incomplete CH$_4$-elimination products including the unreacted neutral ligand. The scaled-up 1:1 ratio reaction in refluxing toluene gave formally diamido−amino aluminum methyl **3** in low yield (23%), but a similar reaction using the *N*-benzyl-substituted ligand HC[SiMe$_2$NH(CH$_2$Ph)]$_3$ afforded the analogous complex **4** in high yield (83%), Scheme 3. The VT NMR spectra from −70 to +60 °C (see Experimental Section) indicated it is fluxional in solution. Attempts to eliminate the third equivalent of CH$_4$ from either **3** or **4** under high-vacuum and -temperature (100−200 °C) conditions were unsuccessful. Treatment of HC[SiMe$_2$NH(4-MeC$_6$H$_4$)]$_3$ with excess of AlMe$_3$ afforded formally amido−amino aluminum dimethyl **5** (Scheme 4); the same strategy was utilized for the preparation of analogous complex **6** bearing the neopentane backboned ligand, MeC[CH$_2$NH-(SiMe$_3$)]$_3$, as its reaction with 1 equiv of AlMe$_3$ in toluene led to a complex mixture.

Besides NMR and analytical characterizations of these aluminum complexes, one monomethyl Al complex (**4**, Figure

(25) Zhu, H.; Chai, J.; He, C.; Bai, G.; Roesky, H. W.; Jancik, V.; Schmidt, H.-G.; Noltemeyer, M. *Organometallics* **2005**, *24*, 380−384.

(26) (a) Gade, L. H. *Eur. J. Inorg. Chem.* **2002**, 1257−1268. (b) Memmler, H.; Kauper, U.; Gade, L. H.; Stalke, D. *Organometallics* **1996**, *15*, 3637−3639. (c) Hellmann, K. W.; Gade, L. H.; Gevert, O.; Steinert, P.; Lauher, J. W. *Inorg. Chem.* **1995**, *34*, 4069−4078.

(27) Forcato, M.; Lake, F.; Blazquez, M. M.; Renner, P.; Crisma, M.; Gade, L. H.; Licini, G.; Moberg, C. *Eur. J. Inorg. Chem.* **2006**, 1032−1040.

(28) The study of the reaction of triaminophosphines P(CH$_2$NHAr)$_3$ with AlMe$_3$ was reported: Han, H.; Johnson, S. A. *Organometallics* **2006**, *25*, 5594−5602.

Scheme 4

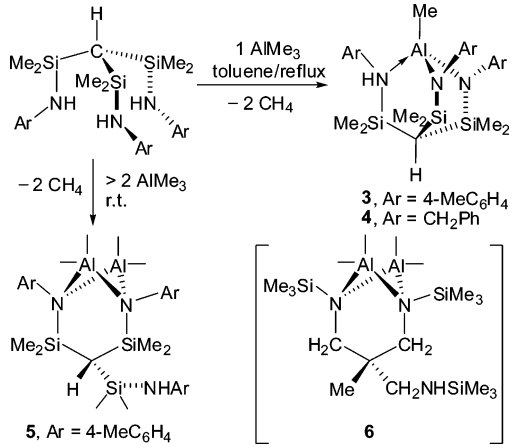

Scheme 5

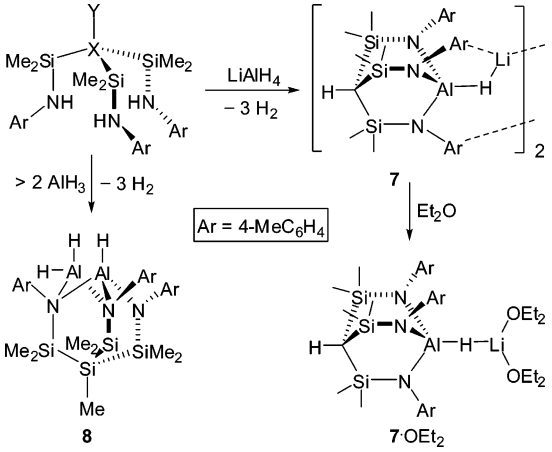

2) and one dimethyl dinuclear Al complex (**5**, Figure 3) were further characterized by X-ray crystallography. The undeprotonated donor amine arm is datively bonded to the Al center in **4**, whereas in **5** it is resided alone. The Al−Me bond length in **4** [1.965(2) Å)] compares well to those in **5** [1.965(3)−1.976-

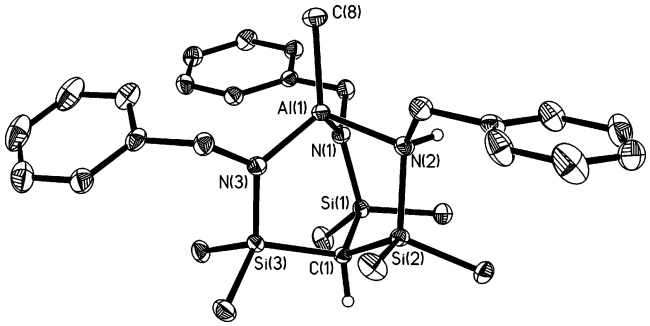

Figure 2. X-ray crystal structure of **4** with thermal ellipsoids drawn at the 50% probability. Selected bond lengths (Å) and angles (deg): Al(1)−C(8), 1.965(2); Al(1)−N(1), 1.840(1); Al(1)−N(2), 2.044(1); Al(1)−N(3), 1.835(1); N(1)−Al(1)−N(2), 98.5(1); N(1)−Al(1)−N(3), 111.8(1); N(2)−Al(1)−N(3), 102.0(1); N(1)−Al(1)−C(8), 114.4(1); N(2)−Al(1)−C(8), 108.1(1); N(3)−Al(1)−C(8), 119.0(1).

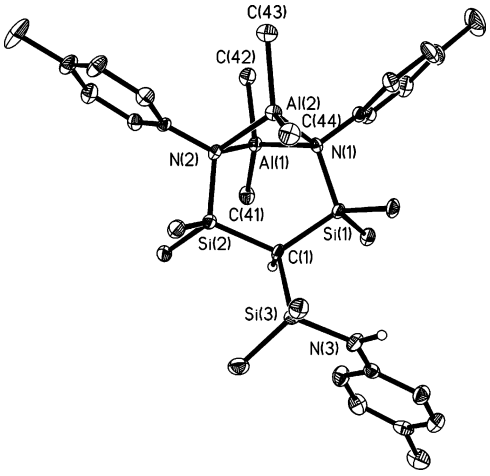

Figure 3. X-ray crystal structure of **5** with thermal ellipsoids drawn at the 50% probability. Selected bond lengths (Å) and angles (deg): Al(1)−N(1), 1.961(2); Al(1)−N(2), 1.980(2); Al(2)−N(1), 1.984(2); Al(2)−N(2), 1.988(3); Al(1)−C(41), 1.969(3); Al(1)−C(42), 1.969(3); Al(2)−C(43), 1.976(3); Al(2)−C(44), 1.965(3); N(1)−Al(1)−N(2), 84.4(1); N(1)−Al(2)−N(2), 83.6(1); C(41)−Al(1)−C(42), 112.1(1); C(43)−Al(2)−C(44), 111.3(1).

(3) Å], and they all are similar to those found in the other four-coordinate aluminum methyl complexes {(±)-*trans*-Cy-(NSiMe$_3$)$_2$}Al$_2$Me$_4$ [1.954(4)−1.964(3) Å][13f] and HC[(CMe)-(NAr)]$_2$AlMe$_2$ [Ar = 2,6-^{i}PrC$_6$H$_3$, 1.955(4)−1.961(3) Å; Ar = 4-MeC$_6$H$_4$, 1.958(3)−1.970(3) Å].[29] The dative Al−N bond in **4** [2.044(1) Å] is longer than those of σ-bonded ones [1.835-(1), 1.840(1) Å]; however, all the Al−N bonds in **5** have similar lengths [1.961(2)−1.988(3) Å)]. It can be seen from Figure 3 that in **5** the two side arrangements of the C−H bond and the free C−SiMe$_2$NH(4-MeC$_6$H$_4$) arm at the apical C atom toward the chelating moiety C[SiMe$_2$N(4-MeC$_6$H$_4$)]$_2$(AlMe$_2$)$_2$ give rise to nonequivalent steric environments for the two bridging AlMe$_2$ moieties; this explains the observed well-separated AlMe$_2$ ^{1}H NMR resonances at −0.21 (s, 3H), −0.18 (s, 3H), and −0.52 (s, 6H) ppm for **5** as well as 0.12 (s, 3H), −0.15 (s, 3H), −0.40 (s, 3H), and −0.59 (s, 3H) ppm for **6**.

Next, we investigated the *H$_2$-elimination* approach using reagents LiAlH$_4$ and AlH$_3$ to react with the neutral ligand [N$_3$]H$_3$ and found that these reagents can completely deprotonate all three amine arms, affording complexes **7** and **8**, respectively (Scheme 5). Addition of Et$_2$O readily converted **7** to its ether adduct. A 3-fold symmetric ^{1}H NMR resonance profile was observed for **7** and **7**·(Et$_2$O)$_2$ in C$_6$D$_6$ at room temperature, but not for **8**. The coordination of Et$_2$O to Li in **7**·(Et$_2$O)$_2$ led to the change of an AB spin splitting pattern for the Ar protons in **7** to a typical AX(M) pattern for the structures without Li−Ar coordination, implying interaction between Li and Ar in **7** but not in **7**·(Et$_2$O)$_2$. A similar observation has been discussed for {HC[SiMe$_2$N(4-MeC$_6$H$_4$)]$_3$Al·ClLi}$_2$ vs its ether adduct HC-[SiMe$_2$N(4-MeC$_6$H$_4$)]$_3$Al·ClLi(Et$_2$O)$_2$.[4a] The reaction of [N$_3$]H$_3$ and AlH$_3$ requires more than 1 equiv of AlH$_3$ for obtaining a clean product (**8**) as the 1:1 ratio led to an unidentifiable mixture even under refluxing conditions, while excess AlH$_3$ (>2) still produced **8**. Treatment of **8** under vacuum at elevated temperatures did not remove one molecule of AlH$_3$ to the desired [N$_3$]Al.

The X-ray diffraction analysis of **8** confirms an unsymmetric tripodal amido dinuclear aluminum hydride structure (Figure 4). One AlH moiety sits in the triamido binding pocket, while the AlH$_2$ moiety is bonded to two diamido N atoms. Both Al centers adopt a distorted tetrahedral geometry with Al−H bond lengths [1.41(5)−1.51(4) Å] within a range observed for terminal aluminum hydrides [1.37−1.75) Å].[30,31] The shortest

(29) Qian, B.; Ward, D. L.; Smith, M. R., III. *Organometallics* **1998**, *17*, 3070−3076.

(30) Gardiner, M. G.; Lawrence, S. M.; Raston, C. L. *J. Chem. Soc., Dalton Trans.* **1996**, 4163−4169.

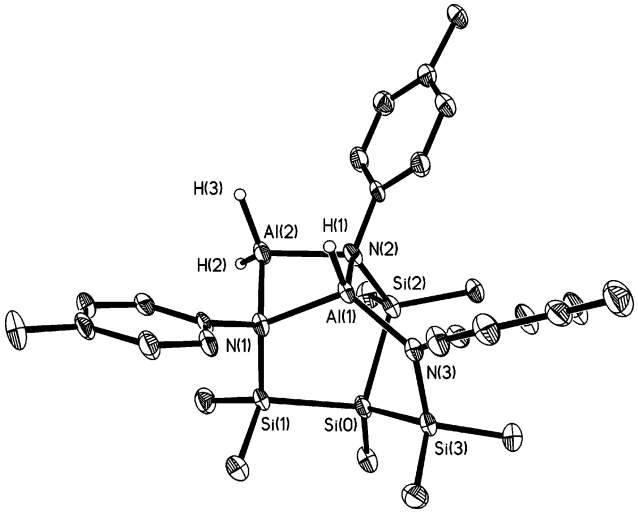

Figure 4. X-ray crystal structure of **8** with thermal ellipsoids drawn at the 50% probability. Selected bond lengths (Å) and angles (deg): Al(1)−N(1), 1.997(3); Al(1)−N(2), 1.965(4); Al(1)−N(3), 1.842(4); Al(2)−N(1), 1.997(4); Al(2)−N(2), 1.955(4); Al(1)−H(1), 1.44(4); Al(2)−H(2), 1.41(5); Al(2)−H(3), 1.51(4); N(1)−Al(1)−N(2), 86.3(2); N(1)−Al(1)−N(3), 120.5(2); N(2)−Al(1)−N(3), 113.8(2); H(1)−Al(1)−N(1), 103.0(16); H(1)−Al(1)−N(2), 116.0-(15); H(1)−Al(1)−N(3), 114.2(15); N(1)−Al(2)−N(2), 86.6(2); H(2)−Al(2)−H(3), 120.0(30).

Scheme 6

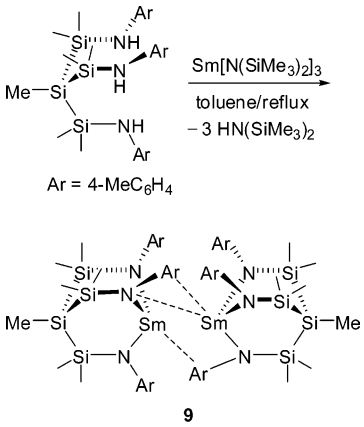

Al−N bond length of 1.842(4) Å is the bond between Al and the only three-coordinate N(3), while the Al to other four-coordinate N (edge-shared diamido N atoms) bonds are >0.1 Å longer [1.955(4)−1.997(4) Å] and still comparable to those found in complexes **4** and **5**. It can be argued that, in view of this structure, the formation of **8** may go through an initial elimination of 2 H_2 by 1 equiv of AlH_3 to give $[N_3H]AlH$ analogous to complex **4**, followed by further elimination of the third H_2 from $[N_3H]AlH$ by an additional equiv of AlH_3.

In addition to the above-described CH_4- and H_2-eliminiation routes, we also examined the *amine elimination* approach using $Al[N(SiMe_3)_2]_3$ to react with the neutral ligand $MeSi[SiMe_2NH(4\text{-}MeC_6H_4)]_3$, but we found no reaction took place even in refluxing toluene. However, this amine elimination route led to the synthesis of the first lanthanide complex (**9**, Scheme 6) incorporating the tripodal triamido ligand. Specifically, the reaction of $Sm[N(SiMe_3)_2]_3$ and $MeSi[SiMe_2NH(4\text{-}MeC_6H_4)]_3$ in toluene under refluxing conditions afforded **9** in 77% yield. As expected, this paramagnetic species gives broad ^1H NMR resonances in C_6D_6 at ambient temperature.

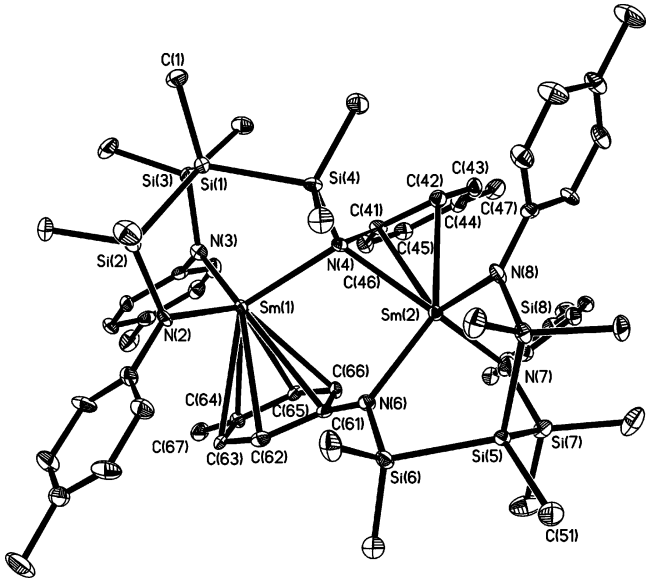

Figure 5. X-ray crystal structure of **9** with thermal ellipsoids drawn at the 40% probability. Selected bond lengths (Å) and angles (deg): Sm(1)−N(2), 2.235(10); Sm(1)−N(3), 2.239(10); Sm(1)−N(4), 2.506(9); Sm(1)−C(61), 2.855(11); Sm(1)−C(62), 2.880(11); Sm(1)−C(63), 2.967(11); Sm(1)−C(64), 3.039(12); Sm(1)−C(65), 2.934(11); Sm(1)−C(66), 2.834(11); Sm(2)−N(4), 2.542(10); Sm(2)−N(6), 2.344(10); Sm(2)−N(7), 2.243(11); Sm(2)−N(8), 2.264(10); Sm(2)−C(41), 2.801(10); Sm(2)−C(42), 2.883(12); N(2)−Sm(1)−N(3), 106.4(4); N(2)−Sm(1)−N(4), 118.1(3); N(3)−Sm(1)−N(4), 103.0(3); Sm(1)−N(4)−Sm(2), 113.9(3); N(6)−Sm-(2)−N(7), 95.0(4); N(6)−Sm(2)−N(8), 118.5(4); N(7)−Sm(2)−N(8), 103.4(4).

The molecular structure of **9** was characterized by X-ray diffraction, featuring an unsymmetric dinuclear structure (Figure 5). The complete elimination of 3 equiv of $HN(SiMe_3)_2$ settles the Sm center nicely above the tripodal binding pocket σ-bound to the three amido N atoms. Due to the low coordination number environment provided by the tripodal triamido ligand and high coordination nature of the 4f block Sm center, further intermolecular interactions of the Sm center with donor groups of another ligand moiety render a dinuclear structure. Sm(1) sits above the $[N_3]$ plane by 0.7803 Å with the $Sm-N_{terminal}$ bonds [2.235(10) and 2.239(10) Å] being shorter than the $Sm-N(4)_{bridging}$ bond [2.506(9) Å], both within a range found for terminal [2.110(10)−2.371(5) Å] and bridging [2.430(10)−2.574(3) Å] amido Sm(III) complexes.[32] This Sm atom is additionally coordinated to an aryl ring from the different tripodal ligand in an η^6-fashion, with the $Sm(1)-C(Ar)_{N(6)}$ distances ranging from 2.834(11) to 3.039(12) Å (av. 2.924 Å), which are compared with those found in complexes $(\eta\text{-}C_6Me_6)Sm(AlCl_4)_3$ (av. 2.89 Å),[33] $(\eta\text{-}C_6H_6)Sm(AlCl_4)_3$ (av. 2.91 Å),[34] $(\eta\text{-}1,3\text{-}Me_2C_6H_4)Sm(AlCl_4)_3$ (av. 2.90 Å),[35] and $(ArO)_6Sm_2$ [Ar

(31) (a) Zhu, H.; Yang, Z.; Magull, J.; Roesky, H. W.; Schmidt, H.-G.; Noltemeyer, M. *Organometallics* **2005**, *24*, 6420−6425. (b) Zhu, H.; Chai, J.; Roesky, H. W.; Noltemeyer, M.; Schmidt, H.-G.; Vidovic, D.; Magull, *J. Eur. J. Inorg. Chem.* **2003**, 3113−3119. (c) Bauer, T.; Schulz, S.; Hupfer, H.; Nieger, M. *Organometallics* **2002**, *21*, 2931−2939. (d) Wehmschulte, R. J.; Power, P. P. *Inorg. Chem.* **1996**, *35*, 3262−3267. (e) Cowley, A. H.; Isom. H. S.; Decke, A. *Organometallics* **1995**, *14*, 2589−2592. (f) Linti, G.; Nöth, H.; Rahm, P. *Z. Naturforsch., B: Chem. Sci.* **1988**, *43*, 1101−1112.

(32) For selected examples, see: (a) Sundermeyer, J.; Khvorost, A.; Harms, K. *Acta Crystallogr.* **2004**, *E60*, m1117−m1119. (b) Martin-Vaca, B.; Dumitrescu, A.; Gornitzka, H.; Bourissou, D.; Bertrand, G. *J. Organomet. Chem.* **2003**, *682*, 263−266. (c) Click, D. R.; Scott, B. L.; Watkin, J. G. *Chem. Commun. (Cambridge)* **1999**, 633−634. (d) Minhas, R. K.; Ma, Y.; Song, J.-I.; Gambarotta, S. *Inorg. Chem.* **1996**, *35*, 1866−1873.

= 2,6-^{i}Pr$_2$C$_6$H$_3$, 2.847(8)−3.135(8) Å, 2.842(7)−3.160(8) Å].[36] The Sm(2) center is located above the [N_3] plane by 0.8822 Å with Sm−$N_{terminal}$ bond lengths of 2.243(11), 2.264(12), and 2.344(10) Å and further coordinated to N(4) and the N(4)-substituted aryl group of the tripodal ligand moiety from another molecule. The Sm(2)−$N(4)_{bridging}$ bond length is 2.542(10) Å, while the Sm(2)−$C(Ar)_{N(4)}$ distances can be divided into two groups: the distances of 2.801(10) and 2.883(12) Å for the Sm(2)−C(41) and Sm(2)−C(42) bonds, respectively, are comparable to the Sm(1)−$C(Ar)_{N(6)}$ distances, while the separations of the others are significantly larger (3.743−4.649 Å), clearly indicating the Sm(2)−$C(Ar)_{N(4)}$ interaction in an η^2-fashion. A comparable case has been observed in compound [$(C_5Me_5)_2$-Sm]$_2$(μ−η^2:η^4-CH_2CHPh).[37] Overall, complex **9** represents an interesting structure model in which the holding of Sm^{3+} under the [N_3] binding pocket and tunable *N*−Ar substituents allow for the presence of intermolecular metal−arene interactions via different bonding modes. These structural features indicate a highly unsaturated Sm center in "[N_3]Sm" supported by the tripodal triamido ligand and reflect the characteristics of the highly electropositive, large Sm center being able to support high coordination numbers.[38]

Ligand Exchange Route. While conventional routes have failed to produce the strongly Lewis acidic alane Al(C_6F_5)$_3$, the facile Al/B alkyl/aryl ligand exchange reaction between $AlMe_3$ and B(C_6F_5)$_3$ has been successful in the high-yield synthesis of this compound.[39] Further studies showed that this ligand exchange reaction proceeds via a stepwise fashion through various boron and mono- or dinuclear aluminum intermediates,[40] and additional procedures such as precipitation of the final product Al(C_6F_5)$_3$ by adjusting the solvent polarity (e.g., use a 1:3 toluene−hexane solvent mixture)[41] are necessary to shift the multiequilibria present in this reaction to the clean alane product.

By analogy, we treated the tripodal borane **A** (*X* = C, *Y* = H, Scheme 1) with $AlMe_3$ in hope of producing the corresponding tripodal alane [N_3]Al. However, this ligand exchange reaction gave a species of non-3-fold symmetry in solution by an observation of two sets of resonances for the 4-*Me*C_6H_4 methyl protons [2.11 (s, 3H) and 2.05 (s, 6H)] and four different $SiMe_2$ methyl resonances [0.46 (s, 6H), 0.44 (s, 6H), 0.29 (s, 3H), and 0.08 (s, 3H)]. There are still two methyl groups attached to Al, indicating the exchange reaction took place only for the first step, which is consistent with the observation of one B*Me* group [0.35 (s, 3H)]. Furthermore, the observed nonequivalency of these two Al*Me*$_2$ methyl groups [−0.49 (s, 3H), −0.53 (s, 3H)] suggests that the Al*Me*$_2$ is coordinated to an additional *N* atom in the resulting ligand exchange product

Scheme 7

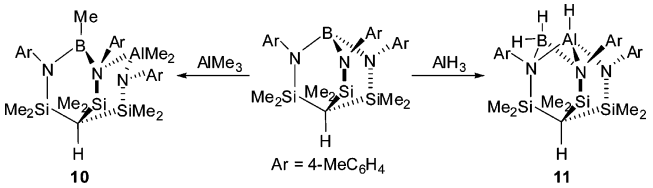

10 (Scheme 7). A most useful, sensitive ^{1}H NMR feature for identifying if the tripodal triamido ligand framework is furnished (i.e., all three amido nitrogen atoms are chelated to a central atom as shown in structures **A** and **B**) or not is the chemical shift of the apical C*H* for the complexes incorporating the tripodal triamido ligand HC[$SiMe_2$N(4-MeC_6H_4)]$_3$: *without exception*, we found that upon furnishing the tripodal geometry, there is a significant upfield shift from the neutral ligand (0.88 ppm) to −0.23 in **A**, −0.46 in **B**, −0.36 in **1**, −0.76 in **3**, −0.95 in **4**, and −0.77 ppm in **7**, while this apical C*H* is located at a downfield region when such a tripodal framework was not established (e.g., 1.11 ppm in **5**). The chemical shift of the apical C*H* in **10** is 1.66 ppm, consistent with the nontripodal structure **10** depicted in Scheme 7.

Interestingly, the ligand exchange reaction between the tripodal borane **A** and AlH_3 produced a second-step ligand exchange product (i.e., a BR_2···AlR type structure), complex **11** (Scheme 7). Using the same analysis as already discussed above, complex **11** retains the tripodal triamido framework as the chemical shift of its apical C*H* is −0.93 ppm. Moreover, the ^{1}H NMR profile of **11** is similar to that of the structurally characterized **8**, implying isostructure of each other. Further treatment of **11** under high-vacuum and -temperature conditions did not drive the reaction to form the third-step ligand exchange product [N_3]Al.

Ligand Redistribution Reaction. A potential application of the preorganized pyramidal tripodal triamido borane [N_3]B is its use as a cocatalyst for metallocene-catalyzed olefin polymerization. To this end, we examined activation of prototypical dimethyl metallocenes Cp_2ZrMe_2 and *rac*-Et(Ind)$_2$$ZrMe_2$ by HC[$SiMe_2$N(4-MeC_6H_4)]$_3$B (**A**: *X* = C, *Y* = H, Scheme 1). Monitoring of the 1:1 molar ratio reactions of both metallocene dimethyls with **A** by ^{1}H NMR in C_6D_6 at room temperature revealed rapid reactions as indicated by the instantaneous disappearance of precursory L$ZrMe_2$ methyl resonances [L = Cp_2, −0.12 ppm; *rac*-Et(Ind)$_2$, −0.95 ppm] and the appearance of resonances assigned to B*Me* and Zr*Me* (0.31 and 0.05 ppm for **12**; 0.21 and −0.67 ppm for **13**, Scheme 8). These spectroscopic features imply the rapid metallocene methide abstraction by the borane. However, the resulting products (from either the NMR-scale reaction or scaled-up isolation) exhibit excellent solubility in hydrocarbons (hexanes, benzene, and toluene), two types of the 4-*Me*C_6H_4 methyl groups [2.18 (s, 3H), 2.13 (s, 6H) for **12**, 2.13 (s, 3H), 2.11 (s, 6H) for **13**], downfield apical *H*C protons (0.50 and 0.56 ppm for **12** and **13**, respectively], and downfield *B*Me resonances in ^{11}B NMR (35.0 and 37.1 ppm for **12** and **13**, respectively]. These lines of evidence point to the neutral species structures with the dismantled tripodal ligand, presumably derived from the initial methide abstraction followed by the amido group transfer from the transient anionic borate center to the cationic zirconocenium center, giving rise to the final neutral species. On the other hand, the weaker Lewis acid MeSi[$SiMe_2$N(4-MeC_6H_4)]$_3$B (**A**: *X* = Si, *Y* = Me, Scheme 1) showed no reaction with Cp_2ZrMe_2 and *rac*-Et(Ind)$_2$$ZrMe_2$. Overall, the facile ligand back-transfer observed for the current tripodal borane system further highlights

(33) Cotton, F. A.; Schwotzer, W. *J. Am. Chem. Soc.* **1986**, *108*, 4657−4658.
(34) Fan, B.; Shen, Q.; Lin, Y. *J. Organomet. Chem.* **1989**, *377*, 51−58.
(35) Fan, B.; Shen, Q.; Lin, Y. *J. Organomet. Chem.* **1989**, *376*, 61−66.
(36) Barnhart, D. M.; Clark, D. L.; Gordon, J. C.; Huffman, J. C.; Vincent, R. L.; Watkin, J. G.; Zwick, B. D. *Inorg. Chem.* **1994**, *33*, 3487−3497.
(37) Evans, W. J.; Ulibarri, T. A.; Ziller, J. W. *J. Am. Chem. Soc.* **1990**, *112*, 219−223.
(38) Edelmann, F. T.; Freckmann, D. M. M.; Schumann, H. *Chem. Rev.* **2002**, *102*, 1851−1896.
(39) (a) Lee, C. H.; Lee, S. J.; Park, J. W.; Kim, K. H.; Lee, B. Y.; Oh, J. S. *J. Mol. Catal., A: Chem.* **1998**, *132*, 231−239. (b) Biagini, P.; Lugli, G.; Abis, L.; Andreussi, P. U.S. Pat. 5,602,269, 1997.
(40) Klosin, J.; Roof, G.; Chen, E. Y.-X.; Abboud, K. A. *Organometallics* **2000**, *19*, 4684−4686.
(41) Feng, S.; Roof, G. R.; Chen, E. Y.-X. *Organometallics* **2002**, *21*, 832−839.

Scheme 8

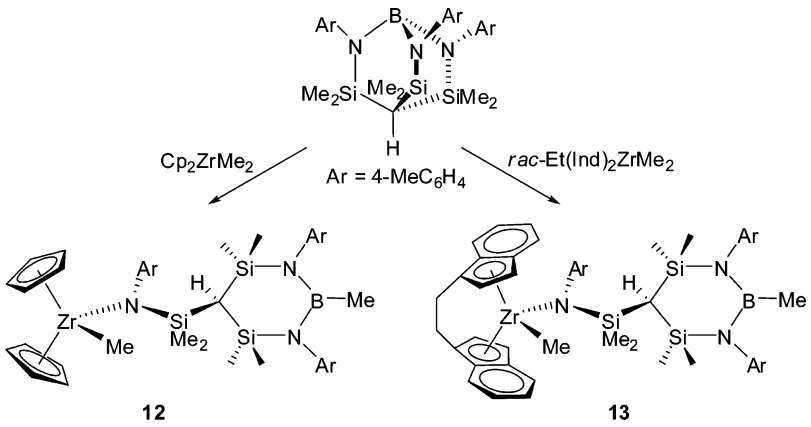

the importance for having the chemical robustness (minimal nucleophilicity or basicity) of the resulting anion when paired with highly electrophilic metallocenium cations.[2d]

The molecular structure of **13** was confirmed by X-ray diffraction analysis, featuring the neutral methyl zirconocene amido species in which the original tripodal framework has been dismantled to the dichelating bis(amido) boron methyl moiety (Figure 6). The three-coordinate B center was formed in a triangular geometry with a perfect plane [B(1)N(2)N(3)C(41) (Δ= 0.0054 Å) and 360.0(4)° peripheral angles around B]. The B−N bonds [1.443(5) and 1.448(6) Å)] are slightly shorter than those in [N_3]B [1.459(2)−1.469(2) Å)],[4a] and the peripheral angles around N(2) and N(3) are 359.6(3) and 358.6(3)°, respectively. These metrical parameters indicate significant π-interactions over the B−N bonds in comparison to those in [N_3]B. The Zr−C bond distance [2.282(4) Å] in **13** compares well with a value of 2.270(7) Å found in another monomethyl derivative *rac*-Et(Ind)$_2$ZrMe[OC(NMe$_2$)═CMe$_2$].[42] The Zr−N bond [2.127(4) Å] is noticeably longer than those found in *rac*-Et(Ind)$_2$Zr(NMe$_2$)$_2$ [2.061(8) and 2.053(9) Å],[23] while the Zr−$C_{centoid}$ separations (2.289 and 2.311 Å) are comparable with values of 2.307 and 2.319 Å observed in *rac*-Et(Ind)$_2$Zr-(NMe$_2$)$_2$.[23]

Polymerization Catalysis. Activation of Cp$_2$ZrMe$_2$ and *rac*-Et(Ind)$_2$ZrMe$_2$ with tripodal borane HC[SiMe$_2$N(4-MeC$_6$H$_4$)]$_3$B gave inactive species for ethylene or propylene polymerization. The inactivity is due to the facile ligand redistribution reaction leading to neutral complexes **12** and **13**, rather than the suspected

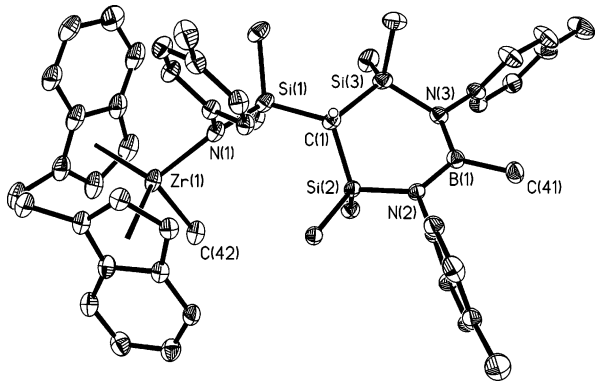

Figure 6. X-ray crystal structure of **13** with thermal ellipsoids drawn at the 30% probability. Selected bond lengths (Å) and angles (deg): Zr(1)−$C_{C5\ ring}$, 2.606(4) (av) and 2.590(4) (av); Zr(1)−C(42), 2.282(4); Zr(1)−N(1), 2.127(4); B(1)−N(2), 1.443(5); B(1)−N(3), 1.448(6); B(1)−C(41), 1.574(6); N(1)−Zr(1)−C(42), 98.8(2); N(2)−B(1)−N(3), 118.1(4); N(2)−B(1)−C(41), 120.9(4); N(3)−B(1)−C(41), 121.0(4).

Table 2. Results of ϵ-CL Polymerization by Tripodal Amido Aluminum Complexes[a]

run no.	[N_3]Al complex	BnOH (equiv)	solvent (mL)	time (min)	yield (%)	M_n[b] (kg/mol)	MWD[b] (M_w/M_n)
1	**1**	0	TOL (3)	40[c]	46	48.6	2.59
2	**1**	0	DCM (5)	60	9	30.4	1.99
3	**1**	1	DCM (5)	60	34	7.12	1.12
4	**1**	10	DCM (5)	60	0		
5	**8**	0	TOL (3)	5[c]	>99	51.3	2.16
6	**8**	0	DCM (5)	120	93	57.2	1.77
7	**8**	1	DCM (5)	60	93	13.6	1.23
8	**8**	10	DCM (5)	60	72	2.98	1.13

[a] Carried out in toluene (TOL) or CH_2Cl_2 (DCM) at 23 °C; 22.5 μmol of the [N_3]Al complex; 200 equiv of ϵ-CL. [b] Number average molecular weight (M_n) and molecular weight distribution (MWD) determined by GPC relative to PMMA standards in $CHCl_3$. [c] Gelation time.

insufficient Lewis acidity of this tripodal borane itself. We also examined ROP of propylene oxide (PO) by selected tripodal borane and alanes, including structures **A**, **B**, and **1**, in the absence and presence of the 1,4-butandiol initiator; however, monomer conversions of these polymerizations were typically below 5% in a 5000/1 [PO]/[catalyst] ratio for 2 h reactions at ambient temperature, as compared to a quantitative PO conversion when B(C_6F_5)$_3$ was used as catalyst under identical conditions.

Next, we investigated ROP of CL by tripodal triamido alane **1** and tripodal amido aluminum hydride **8**, the results of which were summarized in Table 2. As can be seen from this table (runs 1, 2), in either toluene or CH_2Cl_2, alane **1** produced high molecular weight (relative to the [CL]/[catalyst] ratio) PCL (M_n = 4.86 × 10^4 or 3.04 × 10^4) but with relatively broad molecular weight distributions (MWD = 2.59 or 1.99), indicative of a nonliving polymerization process. Upon addition of 1 equiv of benzyl alcohol as initiator or chain-transfer reagent (CTR), the same polymerization afforded PCL with considerably lower MW (M_n = 7.12 × 10^3) and much narrower MWD of 1.12 (run 3, Figure 7). An increase in [BnOH] to 10 equiv shut down the activity (run 4), suggesting this tripodal alane cannot tolerate excess benzyl alcohol, thus failing to effect catalytic ROP of CL. Consistent with these polymerization results, the reaction of **1** and 1 equiv of BnOH showed negligible decomplexation of the tripodal ligand, but the use of 10 equiv of BnOH caused ca. 50% decomplexation of the ligand in a few minutes.

In the absence of BnOH or in the presence of 1 equiv of BnOH, tripodal amido aluminum hydride **8** behaved similarly to tripodal alane **1** in ROP of CL but with considerably higher

(42) Mariott, W. R.; Chen, E. Y.-X. *Macromolecules* **2005**, *38*, 6822−6832.

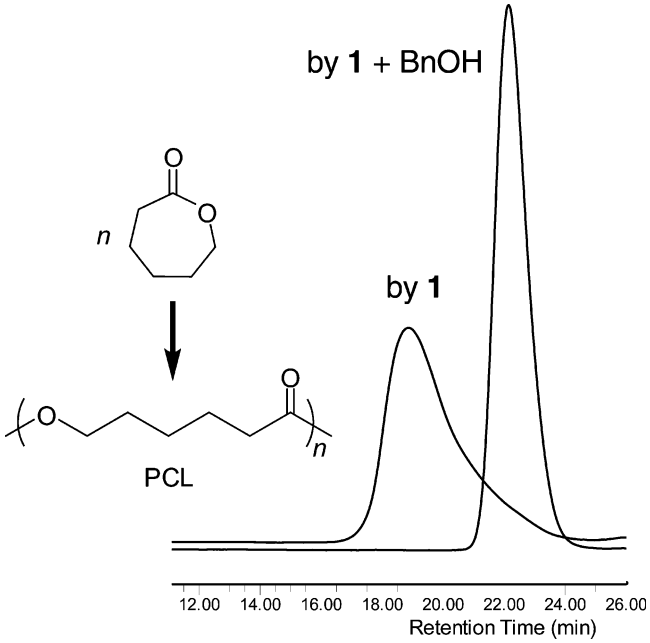

Figure 7. Overlay of GPC traces of PCL produced by tripodal alane **1**. Broad trace: $M_n = 3.04 \times 10^4$, $M_w/M_n = 1.99$ for run 2 in Table 2. Narrow trace: $M_n = 7.12 \times 10^3$, $M_w/M_n = 1.12$ for run 3 in Table 2.

activity (runs 5−7 vs 1−3). More significantly, hydride **8** can tolerate the benzyl alcohol CTR present in large excess (e.g., 10 equiv, run 8), producing PCL with its M_n decreasing as the amount of CTR added increases, characteristic of a chain-transfer polymerization process. For example, when 10 equiv of BnOH was employed (run 8), the resulting PCL exhibits a $M_n = 2.98 \times 10^3$ and $M_w/M_n = 1.13$, calculating to about six polymer chains produced per catalyst center. Consistent with these findings, the reaction of **1** and 1 equiv of BnOH showed negligible decomplexation of the tripodal ligand and that the use of 10 equiv of BnOH led to formation of the Al−OCH_2Ph moiety with the tripodal ligand remaining intact. Overall, these results demonstrate that the aluminum hydride **8** can effect *catalytic* ROP of CL in the presence of CTR.

Conclusions

Overall, by employing several different synthetic strategies described herein we have synthesized a total of 13 new B, Al, and Sm complexes derived from the tridentate tripodal triamine ligand with a neopentane, trisilylmethane, or trisilylsilane backbone and different *N*-substituents; six of these complexes have been structurally characterized by X-ray diffraction studies. We have also investigated the performances of some selected complexes in polymerization of α-olefins, PO, and CL.

The salt-metathesis route involving a lithium salt of the tripodal triamido ligand and $AlCl_3$ requires the use of the preformed THF-solvated Li salt such as $HC[SiMe_2N(CH_2Ph)]_3Li_3(THF)_2$, and the reaction be carried out in a Et_2O/hexanes solvent mixture. Under these conditions, this route readily leads to the formation of complete LiCl-elimination products, tripodal triamido alanes $HC[SiMe_2NAr]_3Al\cdot(THF)$ [Ar = 4-MeC_6H_4,[4a] CH_2Ph (**1**)]. Addition of a small amount of THF to the reaction medium, instead of the use of the preformed THF-solvated Li salt, renders the formation of the THF-ring-opening byproduct $HC[SiMe_2N(4\text{-}MeC_6H_4)]_3Al(OCH{=}CH_2)\cdot Li(THF)_2$.[4a] On the other hand, without using any THF the reaction of $[N_3]Li_3$ in a Et_2O/hexanes solvent mixture produces LiCl-containing compounds such as $HC[SiMe_2N(4\text{-}MeC_6H_4)]_3Al\cdot ClLi(Et_2O)_2$ [4a] and **2**.

The products via the ligand elimination route are sensitive to the reagent MR_3 (M = Al, R = Me, H, $N(SiMe_3)_2$; M = Sm, R = $N(SiMe_3)_2$]. In general, the reaction of $[N_3]H_3$ with 1 equiv of $AlMe_3$ leads to diamido−amino aluminum methyl complexes such as **3** and **4**, while the reaction with ≥2 $AlMe_3$ affords amido−amino aluminum dimethyl complexes such as **5** and **6**. However, none of these methyl aluminum complexes can undergo further elimination of the third equivalent of CH_4 to the still elusive product $[N_3]Al$. The reaction of $[N_3]H_3$ with 1 equiv of AlH_3 gives a complex mixture, but the use of ≥2 AlH_3 leads cleanly to the formation of tripodal dinuclear aluminum hydride **8**. Although there is no reaction between $[N_3]H_3$ and $Al[N(SiMe_3)_2]_3$, this amine-elimination route produces tripodal triamido Sm complex **9** that exhibits a unique dimeric structure in the solid state with intermolecular interactions adopting different metal−arene bonding modes.

The ligand exchange route involves treatment of the tripodal borane $[N_3]B$ with AlR_3 (R = Me, H). The products also depend on AlR_3; while the reaction using $AlMe_3$ stops at the first-step ligand exchange product (**10**), the AlH_3 reagent drives the reaction further to form the second-step ligand exchange product (**11**). The third-step ligand exchange, which is required to occur for obtaining the desired $[N_3]Al$, did not proceed under the present conditions.

The ligand redistribution products are observed when activating dimethyl metallocenes Cp_2ZrMe_2 and *rac*-$Et(Ind)_2ZrMe_2$ with tripodal borane $[N_3]B$. Neutral complexes **12** and **13** are formed presumably via the initial methide abstraction followed by the amido group transfer from the transient anionic borate center to the cationic zirconocenium center. As a result, the "activated" species **12** and **13** exhibit no activity for ethylene or propylene polymerization. This observation further highlights the importance for having the chemically robust anion when paired with highly electrophilic metallocenium cations.

The tripodal triamido alane **1** exhibits low activity for ROP of PO, but moderate activity for ROP of CL. The tripodal aluminum hydride **8** shows much higher activity for ROP of CL than **1**, but more important, **8** effects facile chain-transfer ROP of CL in the presence of benzyl alcohol as CTR for the catalytic production of biodegradable polymer.

Acknowledgment. This work was supported by unrestricted research funds provided by Sumitomo Chemical Co. Ltd. We thank Kazuo Takaoki for ethylene polymerization runs and insightful discussions as well as Susie Miller for the X-ray diffraction data collections.

Supporting Information Available: Crystallographic data for complexes **2**, **4**, **5**, **8**, **9**, and **13**·1.2(hexanes) (CIF). This material is available free of charge via the Internet at http://pubs.acs.org.

OM700587W